Available online at www.sciencedirect.com

ScienceDirect

Geochimica et Cosmochimica Acta 212 (2017) 274–302

Geochimica et Cosmochimica Acta

www.elsevier.com/locate/gca

Stable C, O and clumped isotope systematics and ^{14}C geochronology of carbonates from the Quaternary Chewaucan closed-basin lake system, Great Basin, USA: Implications for paleoenvironmental reconstructions using carbonates

Adam M. Hudson [a,*], Jay Quade [b], Guleed Ali [c], Douglas Boyle [d], Scott Bassett [d], Katharine W. Huntington [e], Marie G. De los Santos [b], Andrew S. Cohen [b], Ke Lin [f], Xiangfeng Wang [f]

[a] *Geosciences and Environmental Change Science Center, U.S. Geological Survey, Lakewood, CO, USA*
[b] *Department of Geosciences, University of Arizona, Tucson, AZ, USA*
[c] *Lamont-Doherty Earth Observatory, Columbia University, Palisades, NY, USA*
[d] *Department of Geography, University of Nevada-Reno, Reno, NV, USA*
[e] *Department of Earth and Space Sciences, University of Washington, Seattle, WA, USA*
[f] *Earth Observatory of Singapore, Nanyang Technological University, Singapore*

Received 22 November 2016; accepted in revised form 15 June 2017; Available online 22 June 2017

Abstract

Isotopic compositions of lacustrine carbonates are commonly used for dating and paleoenvironmental reconstructions. Here we use carbonate $\delta^{13}C$ and $\delta^{18}O$, clumped (Δ_{47}), and ^{14}C compositions to better understand the carbonate isotope system in closed-basin lakes and trace the paleohydrologic and temperature evolution in the Chewaucan closed-basin lake system, northern Great Basin, USA, over the Last Glacial/Holocene transition. We focus on shorezone tufas to establish that they form in isotopic equilibrium with lake water and DIC, they can be dated reliably using ^{14}C, and their clumped isotope composition can be used to reconstruct past lake temperature. Calculations of the DIC budget and reservoir age for the lake indicate residence time is short, and dominated by exchange with atmospheric CO_2 at all past lake levels. Modern lake DIC and shorezone tufas yield $\delta^{13}C$ and ^{14}C values consistent with isotopic equilibrium with recent fossil fuel and bomb-influenced atmospheric CO_2, supporting these calculations. $\delta^{13}C$ values of fossil tufas are also consistent with isotopic equilibrium with pre-industrial atmospheric CO_2 at all shoreline elevations. This indicates that the ^{14}C reservoir effect for this material is negligible. Clumped isotope (Δ_{47}) results indicate shorezone tufas record mean annual lake temperature. Modern (average 13 ± 2 °C) and 18 ka BP-age tufas (average 6 ± 2 °C) have significantly different temperatures consistent with mean annual temperature lowering of 7 ± 3 °C (1 SE) under full glacial conditions. For shorezone tufas and other lake carbonates, including spring mounds, mollusk shells, and ostracod tests, overall $\delta^{13}C$ and $\delta^{18}O$ values co-vary according to the relative contribution of spring and lacustrine end member DIC and water compositions in the drainage system, but specific isotope values depend strongly upon sample context and are not well correlated with past lake depth. This contrasts with the interpretation that carbonate isotopes in closed-basin lake systems reflect changes in DIC and water budgets connected to higher or lower lake volumes. Instead, a small overlapping range of isotope compositions characterize multiple lake levels, so that none can be identified uniquely by isotope composition alone. Relative to other lake carbonates, $\delta^{13}C$ and $\delta^{18}O$ values for ostracods in

* Corresponding author.
E-mail address: ahudson@usgs.gov (A.M. Hudson).

http://dx.doi.org/10.1016/j.gca.2017.06.024
0016-7037/Published by Elsevier Ltd.

Ana River Canyon deposits are very strongly influenced by Ana River water, suggesting low lake level and volume characterized Summer Lake for most of the past 100,000 years. Coupled with sedimentologic observations, the Ana River deposits thus suggest dry conditions like today are close to the mean climate state in the northern Great Basin. By contrast, basin-integrating highstands such as that dating to ~14 ka BP, during the last glacial termination, are hydrologically unique and short-lived. Overall, our results indicate carbonate isotope records must account for the specific geochemical and hydrologic characteristics of lake system in order to provide robust paleoenvironmental reconstructions.
Published by Elsevier Ltd.

Keywords: Great Basin; Closed-basin lake; Clumped isotopes; Carbonate isotopes; Paleoclimate

1. INTRODUCTION

Authigenic carbonate deposits found in closed-basin saline lakes are often used to reconstruct past variability in the lake water environment and by extension, changes in past climate (e.g. Gasse et al., 1991, 1996; Benson et al., 1996a; Cohen et al., 2000; Benson et al., 2003; Jones et al., 2005; Ibarra et al., 2014; Mishra et al., 2015; Petryshyn et al., 2016). Substitutions of stable ^{18}O and ^{13}C and radioactive ^{14}C into the anion (CO_3^{2-}) of $Ca^{12}C^{16}O_3$ are commonly used for paleoenvironmental reconstruction (e.g. Cohen et al., 2000; Benson et al., 2003; Petryshyn et al., 2016) and geochronology (e.g. Broecker and Kaufman, 1965; Hudson et al., 2015; Huth et al., 2015), respectively.

Stable carbon isotope compositions, expressed as $\delta^{13}C$, are useful for reconstructing lake water dissolved inorganic carbon (DIC) composition that is sensitive to biologic productivity (Cohen et al., 2000; Leng and Marshall, 2004) and mixing with atmospheric and groundwater sources of DIC (Nelson et al., 2005). Stable oxygen isotope compositions (expressed as $\delta^{18}O$) in shell materials (e.g. mollusk and ostracod shells) and biologically-mediated authigenic carbonates (e.g. marl, tufas) may provide useful information on variability in the precipitation/evaporation balance of the lake (Leng and Marshall, 2004; Jones et al., 2005; Steinman et al., 2010). In order to derive accurate $\delta^{13}C$ and $\delta^{18}O$ values for past DIC and water from carbonates using temperature-dependent isotope fractionation equations (e.g. Kim and O'Neil, 1997), the temperature of mineral formation must be constrained, which can be difficult for conditions in the geologic past. Clumped isotope thermometry can reduce this uncertainty because the statistical overabundance of ^{18}O-^{13}C bonds in carbonate materials, retained in CO_2 after acid digestion (expressed in per mil as Δ_{47}), varies inversely with formation temperature, and is independent of parent water and DIC isotope composition (Ghosh et al., 2006; Eiler, 2007, 2011). To this end, many empirical temperature-Δ_{47} calibration curves have been generated from both laboratory-precipitated inorganic and biogenic samples as well as with natural geologic samples (Dennis and Schrag, 2010; Quade et al., 2013; Eagle et al., 2013; Zaarur et al., 2013; Tang et al., 2014; Defliese et al., 2015; Kluge et al., 2015; Kele et al., 2015; Kelson et al., 2017; Bonifacie et al., 2017). Building on recent analytical method developments (Daëron et al., 2016; Schauer et al., 2016), new experiments show that a single, robust temperature-Δ_{47} relationship can be used to describe a wide range of natural carbonates (Kelson et al., 2017). In theory, under conditions of isotopic equilibrium between chemical species, stable isotope values for carbonates should be consistent with formation from lake water and DIC isotope values, but offset by the fractionation factors for the temperatures derived from their clumped isotope values. Whether these carbonates form in equilibrium, however, must be tested in order to reconstruct past DIC and water values accurately.

^{14}C in carbonates is often used to provide age control in lake systems (e.g. Benson et al., 2003; Zimmerman et al., 2012; Ibarra et al., 2014), but must be used with caution. ^{14}C dating of Quaternary materials assumes an initial $^{14}C/^{12}C$ ratio equal to that of CO_2 in the atmosphere at the time of formation. However, the stable and radioactive isotope inventories of lacustrine carbonates are inherited from parent water DIC, not just from the atmosphere. Significant errors in ^{14}C age can result where the lake DIC reservoir differs significantly from the atmospheric value at the time of carbonate formation due to mixing with ^{14}C-depleted groundwater, or incomplete mixing with atmospheric CO_2. Therefore, careful consideration of these potential sources of error is required before ^{14}C ages in lacustrine carbonates can be considered reliable. If errors can be minimized or corrected by means of comparison to modern carbonate analogs or other isotopes and dating methods, carbonates can provide valuable age control in closed-basin lake sediments.

We present stable, clumped, U-Th, and radiocarbon isotope data for multiple lake (shorezone and spring mound tufas, mollusk shells, and ostracod valves) and terrestrial (spring travertines) carbonates to improve understanding of the carbonate isotope system and trace the paleohydrologic evolution of the Chewaucan closed-basin lake system in western North America. This lake system is advantageous because it contains a perennial lake and recently deposited carbonates that provide a modern analog for the isotope behavior of the lake during the geologic past. We focus mainly on interpreting stable isotope variations and ^{14}C dates for modern and fossil tufas, with the goal of assessing the accuracy of ^{14}C ages for this material, which is used in this and other studies to reconstruct lake level histories. We also assess modern and past lake surface temperatures based on clumped isotope thermometry. We then examine stable isotope variations in multiple carbonate types to assess the dominant controls on their isotopic compositions and their relationship to lake hydrologic change. Measurements from terrestrial, shorezone, and off-

shore carbonate phases within a single lake system provide useful comparison between lake level variations reconstructed from shoreline sediments and variations in the isotope content of lake water, which are often used in core-based reconstructions to infer lake depth or hydrologic budget.

2. STUDY AREA AND PREVIOUS WORK

The Lake Chewaucan (Cheh-wah-CAN) system is located in southern Oregon, USA (42.7°N, 120.5°W) in the northwestern corner of the Great Basin (Fig. 1). The drainage basin consists of wide playa floors of moderate elevation (1267–1314 m asl; above sea level) surrounded by normal fault-bounded mountain ranges up to 2536 m asl. Located at the intersection of the Basin and Range and the Columbia River Basalt Plateau, the basin bedrock is composed entirely of extensively faulted andesitic and basaltic volcanic rocks of Miocene to Pliocene age (Walker and Macleod, 1991). Quaternary basin deposits underlie the modern basin floor and include interbedded lake silts and evaporites in the Summer Lake and Abert Lake basin centers, marsh peats around the margins and covering the Upper and Lower Chewaucan Marshes, and sand/gravel shoreline deposits defining past and present lake shoreline elevations (Allison, 1982). Significant offset on normal faults cutting Quaternary deposits (Pezzopane and Weldon, 1993) indicates the study area is actively extending.

The Chewaucan hydrographic system is internally drained with no surface water outlet at any paleoshoreline levels. It consists of four sub-basins from west to east: Summer Lake, Upper Chewaucan Marsh, Lower Chewaucan Marsh, and Abert Lake. These basins were variably connected depending on past lake level (Fig. 1). The modern Summer and Abert Lake sub-basins are currently occupied by semi-perennial lakes with areas of approximately 187 and 115 km^2, respectively. The Summer Lake sub-basin has a total area of 1051 km^2, but has a relatively small contributing catchment confined to Winter Ridge on the south and west. The Ana River dominates runoff into the Summer Lake sub-basin. It is sourced from a spring in the northwestern part of the basin, and flows southward through the Ana River Canyon to feed the Summer Lake playa (Phillips and Van Denburgh, 1971).

The other three sub-basins are hydrographically connected today along a set of topographic steps with a total area of 2657 km^2. They are fed from the west by the Chewaucan River, which ends in Abert Lake. The modern river has been diverted into irrigation canals that flow continuously to Abert Lake. However, natural conditions likely supported extensive marshes in the upper sub-basins. There is no indication that these three sub-basins were separated by hydrographic divides in the recent geologic past, so it is convenient to consider them as a single hydrologic unit, called the Abert Lake sub-basin hereafter. The Chewaucan River drains most of high elevation of this sub-basin, with minor seasonal contributions from Willow and Crooked Creeks feeding from high topography along the south side of Lower Chewaucan Marsh (Fig. 1).

There has been a significant amount of prior research conducted on both the modern Summer and Abert Lake sub-basins and the paleolake sediments, including lacustrine carbonates. Allison (1982) provided descriptions of the geomorphology and sedimentology of the alluvial, lacustrine, and landslide deposits within the basin. Previous studies of the water chemistry (Whitehead and Feth, 1961; Van Denburgh, 1975) and hydrologic budgets of the Abert Lake and Summer Lake watersheds (Phillips and Van Denburgh, 1971) have characterized the solute composition and concentrations of the lakes and the contributions of inflowing streams and springs within the historical record. These works provide a valuable framework for interpreting the effect of salinity and solute composition on formation and isotope composition of modern and fossil carbonates in this study.

The most extensive study of lake deposits has focused on fine-grained sediments exposed in deep streamcuts carved by the Ana River in the northern Summer Lake sub-basin (Fig. 1). These exposures in the Ana River Canyon (ARC) have yielded paleoenvironmental records spanning much of the past ~150 ka, based on sedimentology (Allison, 1982; Cohen et al., 2000), paleomagnetic indicators (Negrini et al., 2000; Zic et al., 2002), pollen, and ecology and geochemistry of ostracods (Palacios-Fest et al., 1993). The ARC deposits also contain at least 88 volcanic tephras (summarized by Kuehn and Negrini, 2010) used for geochronology and stratigraphic correlation of sediment records within the Chewaucan lake system and within the northern Great Basin. Ostracod valves have also been used for geochronology and paleotemperature reconstructions using amino acid racemization (Bright and Kaufman, 2011a, 2011b; Reichert et al., 2011).

Two additional core records from the Wetlands Levee (WL) and Bed & Breakfast (B&B) localities in the Summer Lake sub-basin have been correlated to the ARC sections using magnetostratigraphy, tephrostratigraphy and ^{14}C ages on ostracods, and also contain a suite of paleoenvironmental indicators including stable isotope values for ostracods (Cohen et al., 2000; Benson et al., 2003; Fig. 1). The combined records show that lake level and vegetation changes in the catchment generally followed the global glacial-interglacial temperature trend, with cold and/or moist conditions prevailing during Marine Isotope Stages (MIS) 6, 4, and 2. Major unconformities indicated by erosion and eolian deflation of basin sediments developed during the MIS 5 and 1 (Holocene) interglacials, and dry conditions relative to MIS 4 and 2 occurred during MIS 3.

A few studies have targeted shoreline deposits in the Abert Lake sub-basin, where shoreline sediment sequences are well exposed along the base of the Abert Rim (Fig. 1). Jellinek et al. (1996) produced stable isotope values for spring mound and shorezone tufas, concluding the $\delta^{18}O$ values indicated formation in an evaporated closed-basin lake environment. Licciardi (2001) reconstructed lake levels for Abert Lake using ^{14}C dating of lacustrine mollusk shells, identifying a Late Glacial (MIS 2) highstand interval between 13 and 14 cal ka BP. However, the DIC reservoir correction for Abert Lake with respect to ^{14}C has not been

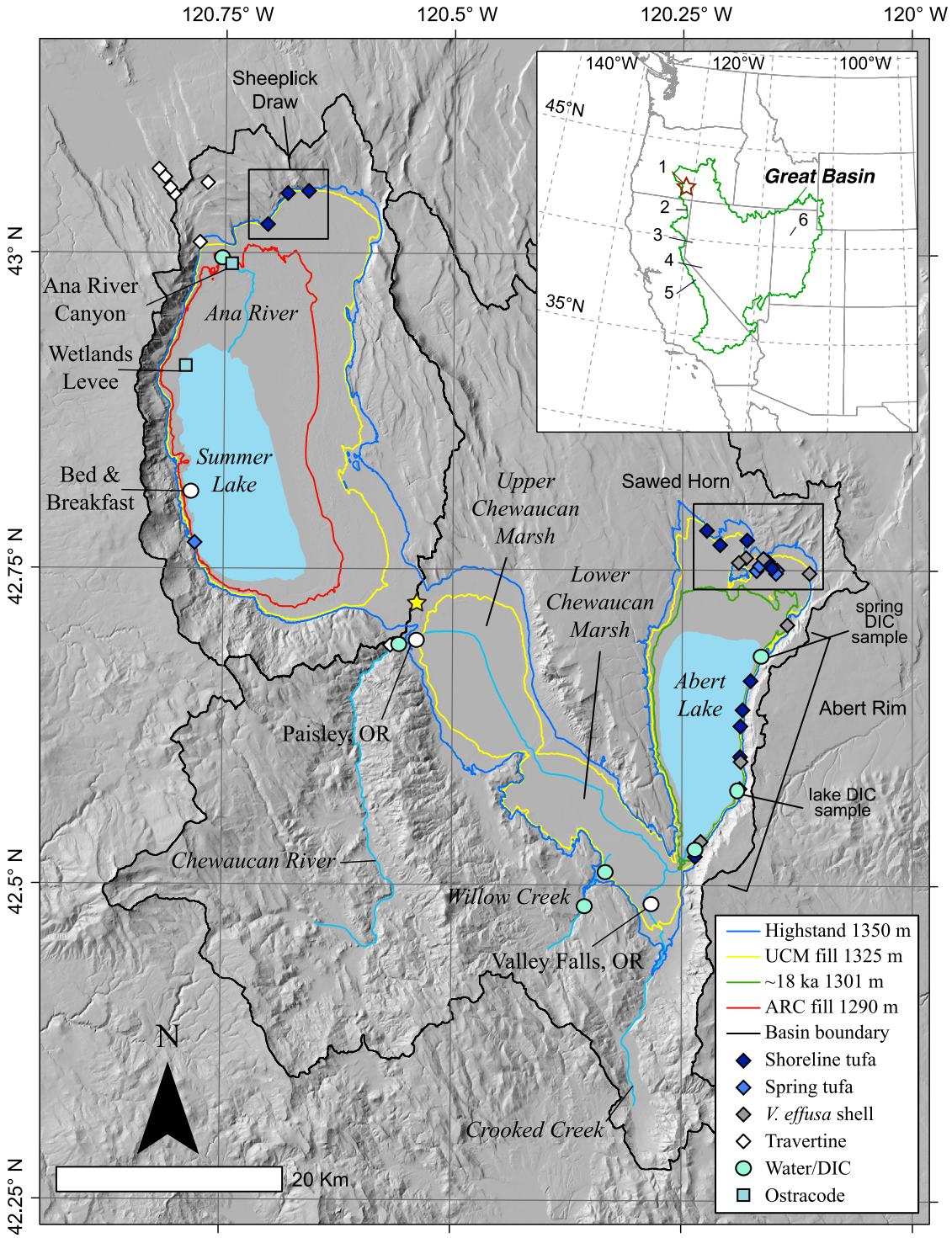

Fig. 1. Chewaucan pluvial lake system. Approximate modern playas of Summer and Abert Lake and modern inflowing rivers shown in light blue. Hydrographic basin boundaries shown in black. Sampling locations are shown by symbols coded by carbonate type. Sampling areas in this study are indicated by black boxes or brackets. Locations of the Ana River Canyon section, and Wetlands Levee and Bed & Breakfast cores are labeled (Cohen et al., 2000). Lake area defined by shorezone tufas of ~18 ka age shown in green; lake area at the elevation filling the Upper Chewaucan Marsh (UCM) in yellow; lake area required to submerge the Ana River Canyon (ARC) sections shown in red; lake area at the Late Glacial high shoreline elevation shown in blue. Location of meteorological station at Valley Falls, OR shown by open circle, and location of spill point between Summer and Abert sub-basins by yellow star. Base image derived from the 10 meter National Elevation Dataset. Inset – western North America map showing study area (red star) and locations of lakes from other studies. Great Basin hydrographic boundary outlined in green. 1 – Lake Chewaucan, 2 – Lake Surprise, 3 – Pyramid Lake, 4 – Walker Lake, 5 – Mono Lake, 6 – Lake Bonneville. (For interpretation of the references to colour in this figure legend, the reader is referred to the web version of this article.)

rigorously considered, and these dates need further assessment.

3. CARBONATE MATERIALS

There are several types of carbonate materials found in the Quaternary deposits of the Chewaucan basin, deposited in both lacustrine and terrestrial (i.e., non-lacustrine) environments (Figs. 1 and 2). For clarity, carbonate deposits associated with spring discharge from subaerially exposed (terrestrial) outlets are referred to as travertines. By contrast, inorganic and/or biologically mediated carbonates formed in a subaqueous (lacustrine) setting are referred to as tufas. Lacustrine shell carbonates include mollusk shells and ostracod valves. Each material is associated with a particular geomorphic and sedimentary setting within the basin, providing potential constraint on the age and past water chemistry in the environment of formation. The materials described here are combined from this study and previous publications, ranging in age from modern to >100 ka BP. We attempt to place coarse age constraints on data from each carbonate type based on previous work and the new dating results for this study.

3.1. Spring travertines

Jellinek et al. (1996) described and produced stable isotope values for spring travertines in the northwestern Summer Lake sub-basin associated with spring discharge localized along small normal faults. Their locations are above and geographically outside the highest studied paleoshorelines of the Chewaucan system (1350 m asl; Fig. 1) and therefore they were deposited in a terrestrial environment. These deposits are of unknown age but are likely Quaternary (Jellinek et al., 1996).

3.2. Shorezone tufas and spring mound tufas

Shorezone tufas are commonly found in shoreline sediments of closed-basin lake systems (e.g. Broecker and Kaufman, 1965; Nelson et al., 2005; Placzek et al., 2006; Ibarra et al., 2014; Hudson et al., 2015). Spring mound tufas are found in association with localized areas of underwater spring discharge into the lakes (e.g. Benson et al., 1996a). Both types are typically cream to white in color and vary widely in texture, from laminar, botryoidal to dendritic. They can form as both calcite and/or aragonite depending upon lake water composition (e.g. Nelson

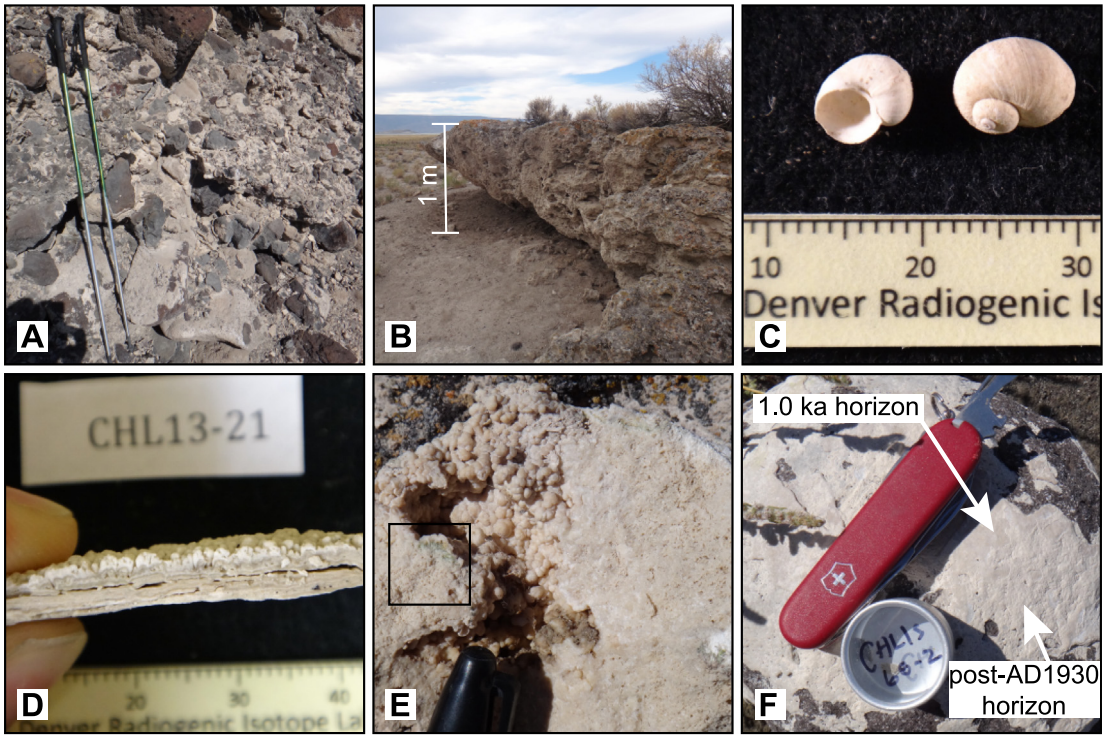

Fig. 2. Field and sample photographs of Chewaucan carbonates. All photo credits: A. Hudson, September 2014 – May 2016. A – tufa-cemented high shoreline (1346–1350 m asl) gravel from Sheeplick Draw locality, north Summer Lake sub-basin. Trekking pole for scale is 130 cm in length. B – spring mound tufa (CHL14-1G, 1307 m asl) from Sawed Horn locality, north Abert Lake sub-basin. C – Fossil *v. effusa* mollusk shells collected from littoral deposits (CHL13-14b, 1326 m asl) in the Sawed Horn locality, north Abert Lake sub-basin. Scale is in mm. D – cross-section of tufa sample (CHL13-21, 1296 m asl) from Abert Rim locality showing lower laminated horizons overlain by upper dendritic horizons. Scale is in mm. E – closeup of spring mound tufa (CHL15-62, 1309 m asl) from Sawed Horn locality showing fibrous carbonate texture with botryoidal texture carbonate deposited in void. Green algal remains at contact between two carbonate types shown by black box. Felt tip pen cap for scale is ~1 cm in width. F – recent-age tufa sample (CHL15-68, 1295 m asl) on beach cobble from Abert Lake playa edge, Abert Rim locality. ~1.0 ka BP laminar tufa horizon overlain by modern laminar tufa horizon indicated by arrows. Pocket knife for scale is ~12 cm in length.

et al., 2005; McGee et al., 2012). X-ray diffraction analysis (XRD) of both shorezone and spring mound tufas for the Chewaucan system indicates they are pure calcite at all shoreline levels.

The general occurrence of shorezone tufas at shallow lake depths (generally <20 m; Brady et al., 2010) and in nearshore and beach deposits, coupled with the common inclusion of algal organic matter within the carbonates, indicates carbonate formation is at least partially biologically mediated by photosynthesis, and hence restricted to the shallow photic zone. This makes shorezone tufas excellent candidates for constraining past lake surface elevations and reconstructing environmental conditions within the lake epilimnion. In the Lake Chewaucan system, shorezone tufas are found in areas with significant modern spring discharge nearby. For this study, they were sampled from shorelines in the Sheeplick Draw, Sawed Horn, and Abert Rim areas on modern and paleoshorelines ranging in elevation from 1295 to 1350 m asl (Fig. 1). They typically occur on cobble to boulder-sized basalt clasts in rocky shoreline deposits, forming coatings <1–30 mm in thickness in sheltered areas (Fig. 2A). These tufas are layered, typically with dense basal laminae coating volcanic clasts, grading upward into more porous, dendritic textures at the top of the deposit (Fig. 2D). Based on previous research (Allison, 1982; Friedel, 2001), and results from this study, these tufas range in age from modern to ~25 ka BP.

Spring mound tufas are found on top of former underwater spring discharge locations, as elongate deposits along small normal faults in the western Summer Lake sub-basin and in the Sawed Horn area of the Abert sub-basin (Fig. 1). In contrast to the shorezone tufas, spring mound tufas form mushroom-shaped mounds approximately 50–200 cm in height deposited on littoral sands and fine gravels distal to the cobble-boulder paleoshorelines (Fig. 2B). The majority of the carbonate is white with a filamentous texture, and poorly stratified. Voids in the porous material contain dense laminar and botryoidal carbonate (Fig. 2E). These deposits are likely >20 ka BP in age, based on our U-Th dating results.

3.3. Mollusk shells

Lacustrine mollusk shells considered in this study are found only in the Lake Abert sub-basin, although Cohen et al. (2000) note the presence of reworked shells in the Ana River Canyon sediments. Allison (1982) also reports fossil shell from the northeastern Summer Lake sub-basin. For consistency, only *Vorticifex effusa* (Fig. 2C), the most common shell found in the deposits of Lake Abert, was sampled for isotope analysis. In this study, all mollusk shells were sampled in shallow water deposits, including littoral sands and gravel beach deposits (Fig. 1). The shells are likely ~13 to 14.5 ka BP in age, based on previous dating (Friedel, 2001; Licciardi, 2001).

3.4. Ostracod valves

The carbonate valves of ostracods are abundant in fine-grained lake deposits in the Great Basin. *Limnocythere ceriotuberosa,* a benthic ostracod with a wide salinity tolerance, occurs almost continuously within these deposits in the Lake Chewaucan system, and was previously targeted for isotope analysis in the ARC, WL and B&B records (Palacios-Fest et al., 1993; Cohen et al., 2000; Benson et al., 2003). For this study, we have compiled published ostracod isotope data from the ARC and WL records (Palacios-Fest et al., 1993) for comparison to other carbonate types presented in this study (Fig. 1). These ostracod valves are constrained by tephrochronological evidence to >20 ka to >150 ka in age, but are mostly within the range ~20 to 100 ka BP (Cohen et al., 2000).

4. METHODS

4.1. Field and laboratory sampling

Carbonates and waters in the study area were described and sampled in 2013–2015. Tufas were sampled *in situ* from bedrock outcrops, tufa mounds, or *in situ* shoreline clasts using a hammer and chisel. Mollusk shells were sampled *in situ* from natural exposures or hand-dug trenches in lake deposits. Waters were sampled unfiltered in 50 mL plastic vials, overfilled to eliminate headspace, sealed with thread-seal tape, and refrigerated until analyzed. Each sample location was recorded using a high-precision differential GPS unit, resulting in 0.4–0.9 m vertical and 0.1–0.3 m horizontal precision.

In the laboratory, tufas were sectioned with a lapidary saw to expose the internal stratigraphy, and individual horizons were sampled using a stationary micro-mill apparatus. Carbonate powders (5–50 mg) were retained for stable and/or clumped isotope analysis, whereas chunks (10–20 mg) were retained for ^{14}C and U-Th series dating.

Subsamples for dating were treated with 2% H_2O_2 for 4 h to remove organic material, soaked overnight, then rinsed thoroughly with distilled water, and dried overnight at 70 °C. Mollusk shells were visually inspected to minimize adhering detritus, then cleaned ultrasonically in distilled water for 15 min, and treated with 2% H_2O_2 and dried as above. Travertines were separated from clasts using dental tools, and cleaned with the same procedure as shells. Single whole shells and other carbonates (5–10 mg) were powdered using an agate mortar and pestle for stable isotope analysis.

The sample fraction used for U-Th dating was further cleaned ultrasonically in ultrapure water. Approximately 2 mg of sample powder was then collected by drilling into the clean surface. U and Th isotope fractions were separated and purified chemically following Cheng et al. (2000).

4.2. Carbonate stable isotope analysis

$\delta^{18}O$ and $\delta^{13}C$ in carbonates ($\delta^{18}O_c$ and $\delta^{13}C_c$) was analyzed by a Kiel III device coupled to a Finnigan MAT 252 mass spectrometer at the University of Arizona. Measured $\delta^{18}O_c$ and $\delta^{13}C_c$ values were corrected using internal laboratory standards calibrated to NBS-19. Precision of repeated standards is ±0.11‰ for $\delta^{18}O_c$ (1σ), and ±0.08‰ for $\delta^{13}C_c$ (1σ). Carbonate isotopic results are

reported using standard δ-per mil notation relative to Vienna Pee Dee Belemnite (VPDB).

4.3. Clumped isotope analysis

Clumped isotope analysis (Δ_{47}) of select shorezone tufa samples was performed at the University of Washington. Carbonate samples and standards (6–10 mg) were digested for 10 min at 90 °C in a common bath of phosphoric acid (specific gravity 1.90–1.95). The evolved CO_2 was cryogenically separated from water and purified on an automated stainless steel and nickel vacuum line, which used He as the carrier gas to pass the CO_2 through a Porapak Q trap (50/80 mesh, 15 cm long, 4.5 mm ID, 0.635 mm OD) held between −10 °C and −20 °C for a transfer time of 15 min. For each four carbonate sample unknowns a carbonate standard was digested and purified using the same procedure. Purified CO_2 was transferred to Pyrex break seals and loaded into an automated 10-port tube cracker inlet system on a Thermo MAT 253 mass spectrometer configured to measure masses 44–49 inclusive. Δ_{47} values were calculated using established methods (Huntington et al., 2009), with the exception that we used the updated ^{17}O correction values recommended by Brand et al. (2010), Schauer et al. (2016) and Daëron et al. (2016). Measurements consisted of 6 acquisitions of 10 cycles each, with a 26 s integration time (Schauer et al., 2016). Δ_{47} values were corrected to the absolute reference frame (ARF) of Dennis et al. (2011) using analyses of CO_2 heated to 1000 °C, and equilibrated with water at 4 and 60 °C. Sample Δ_{48} values were used to screen for contamination ($\Delta_{48} > 2‰$ rejected). Four to six replicate analyses were conducted for each sample. Full data for reference frame gases, carbonate standards, and samples are given in Table S5. Δ_{47} uncertainties are given as one standard error (1 SE) of replicate measurements. Standard errors were calculated using either the standard deviation of sample replicates or the long-term standard deviation of carbonate standards measured at UW Isolab (0.028‰ for Δ_{47}), whichever is greater. Temperature was calculated from sample average Δ_{47} values using the calibration of Kelson et al. (2017; Eq. (2), no acid fractionation), which is based on data for 56 synthetic carbonates digested at 90 °C. We use this temperature calibration because it incorporates the highest number of data, was produced using identical gas preparation and measurement methods to those used in this study, and also applies the isotopic parameters for ^{17}O recommended by Brand et al. (2010). Additional calibrations for inorganic carbonates (Dennis and Schrag, 2010; Zaarur et al., 2013; Tang et al., 2014; Defliese et al., 2015; Kluge et al., 2015; Kele et al., 2015) comprise data that have been calculated using ^{17}O correction parameters based on the quartz-water system (e.g., Santrock et al., 1985), which is known to introduce inaccuracies in Δ_{47} (Daëron et al., 2016; Schauer et al., 2016). For comparison sake, we also calculate our sample temperatures with the previous tufa- and travertine-specific calibration of Kele et al. (2015), using Δ_{47} data from this study recalculated using the Santrock et al. (1985) parameters. The results of this exercise are summarized in Table S3 and differ within error (0–5 °C) from the temperatures reported in Table 3. Insufficient data are available to recalculate previously published calibration samples using the Brand et al. (2010) correction at this time. Therefore when comparing our dataset to previously published Δ_{47} values for tufas that do not incorporate the Brand et al. (2010) correction, we choose to compare directly to the published values and interpretations of those authors. Our data comparison (Table S3) using the two alternative calibration methods indicates this is unlikely to cause significant error.

4.4. Water isotope analysis

$\delta^{18}O$ values of water samples ($\delta^{18}O_w$) were measured using the CO_2 equilibration method on an automated sample preparation device attached directly to a Finnigan Delta S mass spectrometer at the University of Arizona. δD values of water were measured using an automated chromium reduction device (H-Device) attached to the same mass spectrometer. The values were corrected based on internal laboratory standards, which are calibrated to VSMOW and SLAP. The analytical precision for $\delta^{18}O_w$ and δD measurements is 0.08‰ and 0.6‰, respectively (1σ). Water isotopic results are reported using standard δ-per mil notation relative to Vienna Standard Mean Ocean Water (VSMOW).

4.5. Radiocarbon dating

With all dating samples, care was taken to select dense tufa from sample cross-sections, and any outer surfaces exposed to weathering were gently abraded prior to analysis to reduce surface contamination. Previous research shows that younger carbon may be incorporated by subsequent lake carbonate deposition in voids, or by dissolution/precipitation during subaerial weathering after lake recession, resulting in younger ^{14}C ages (e.g. Zimmerman et al., 2012). However, careful sample selection and treatment can drastically reduce potential contamination (Zimmerman et al., 2012; McGee et al., 2012). The most dense materials were sampled and dissolved as 10–20 mg chunks without crushing to minimize area-to-volume ratio, minimizing surface sorption of modern CO_2. No evidence of secondary filling of voids with younger carbonate was observed in any samples. Given these measures, significant young carbon contamination is unlikely in our samples.

Sample tufa chunks were reacted with >100% H_3PO_4 under vacuum until fully dissolved to evolve CO_2 gas. Waters for DIC analysis were acidified with 85% H_3PO_4 under vacuum to evolve all DIC to CO_2. All sample CO_2 was extracted under vacuum, cryogenically purified and passed through a 600 °C Cu/Ag furnace to remove contaminant gases. Purified CO_2 samples were graphitized using 100 mg of zinc powder and Fe powder in a 2:1 proportion to the mass of carbon in the sample. Accelerator Mass Spectrometry (AMS) ^{14}C and $\delta^{13}C$ measurements were performed by the Arizona AMS Laboratory. $\delta^{13}C_c$ values for purified gases for individual samples are statistically indistinguishable from those measured by stable and clumped isotope methods above, and are not reported. Raw ^{14}C isotope ratios are reported as fraction modern carbon

(FMC) relative to the activity of the atmosphere in AD 1950. Raw ^{14}C ages are reported with 1σ error as ^{14}C years before present (^{14}C yr BP), and were calibrated using the OxCal 4.2 software with the IntCal13 calibration curve (Bronk Ramsey, 2009; Reimer, 2013). All calibrated ^{14}C ages are reported in calendar years BP as the median age of the calendar range ± 2σ error.

4.6. U-Th series dating

U and Th sample fractions were measured using a ThermoFisher Neptune Plus multi-collector ICP-MS at the Earth Observatory of Singapore, Nanyang Technological University, Singapore. Ages were calculated using the ^{230}Th ($\lambda_{230} = 9.1705 \times 10^{-6}\ yr^{-1}$) and ^{234}U ($\lambda_{234} = 2.82206 \times 10^{-6}\ yr^{-1}$) half-lives of Cheng et al. (2013) and the ^{238}U ($\lambda_{238} = 1.55125 \times 10^{-10}\ yr^{-1}$) half-life of Jaffey et al. (1971). The detrital/hydrogenous ^{230}Th correction for age calculations assumes the initial atomic ratio of $4.4(\pm 2.2) \times 10^{-6}$ for a material at secular equilibrium with the bulk earth $^{232}Th/^{238}U$ ratio of 3.8. The error in the initial ratio is arbitrarily assumed to be 50%. Previous research indicates that this initial ratio may be lower than that measured for modern high pH salt lakes in the Great Basin, due to hydrogenous Th contribution (Walker Lake, Pyramid Lake, Mono Lake; Lin et al., 1998). However, these $^{230}Th/^{232}Th$ ratios range from ~10 to 16×10^{-6}, much lower than the measured $^{230}Th/^{232}Th$ atomic ratio for the sample in this work ($1.74 \pm 0.07 \times 10^{-3}$; Table S4). This sample is dominated by authigenic ^{230}Th, so that the uncertainty in either detrital or initial ratio should not affect the age by more than ~60 yr. This is less than the uncertainty in the age, and therefore should not affect the date significantly. It is unknown what the initial ratio is in modern Abert Lake, or what it would have been at high lake level, making any alternate detrital/hydrogenous ratio uncertain. The U-Th date is therefore expressed with 2σ uncertainties and was corrected to AD 1950 to be consistent with ^{14}C dates.

Multiple attempts to date shorezone tufas using U-Th series disequilibria yielded high age uncertainties (>3000 yr) due to low U content (averaging $^{238}U = 570 \pm 290$ ppb) and high detrital Th (averaging $^{232}Th = 1420 \pm 2200$ ppb). These samples yielded $^{230}Th/^{232}Th$ atomic ratios of $< 5 \times 10^{-6}$, much too low for accurate dating of lacustrine carbonates (Placzek et al., 2006). Only the spring mound tufa sample ($[^{230}Th/^{232}Th] = 1747 \pm 72 \times 10^{-6}$) was near detritus-free ($^{238}U = 576 \pm 5$ ppb, $^{232}Th = 2.6 \pm 0.1$ ppb) and suitable for single-analysis dating.

5. ISOTOPE AND DATING RESULTS

Our results and those of previous studies span a range of materials and methods, as summarized in Table 1. We have compiled a total of 65 new and 114 previously published stable isotope values for the carbonate materials described above (Table 2, S1). We also present eight new and 134 previously published $\delta^{18}O_w$ and δD values for streams, springs, and lakes within the drainage basin and surrounding region to aid in interpretation of the carbonate $\delta^{18}O_c$ values

Table 1
Sample materials and analyses from the Chewaucan lake system.

Sample material	Elevation range (m asl)	Age range	Lake sub-basin	Formation environment	Analyses	Source
Meteoric Waters	1288–1369 m	Modern	Abert/ Summer	–	Water $\delta^{18}O$, δD; DIC $\delta^{18}O$, $\delta^{13}C$, ^{14}C	Palmer et al. (2007); this study
Spring travertine	>1350 m	Quaternary	Abert/ Summer	Spring discharge outlets, non-lacustrine	Carbonate $\delta^{18}O$, $\delta^{13}C$	Jellinek et al. (1996) this study
Shorezone tufa	1295–1350 m	modern to 25 ka BP	Abert/ Summer	Shorezone, lacustrine	Carbonate $\delta^{18}O$, $\delta^{13}C$, Δ_{47}, ^{14}C	This study
Spring mound tufa	1275–1312 m	>20 ka BP	Abert/ Summer	Underwater spring discharge outlets, lacustrine	Carbonate $\delta^{18}O$, $\delta^{13}C$, ^{14}C, U-Th	Jellinek et al. (1996) this study
Vorticifex effusa shells Ana River Canyon	1302–1346 m 1280 m	13–14 ka BP 20 to >100 ka	Abert Summer	Shorezone, lacustrine Benthic, lacustrine	Carbonate $\delta^{18}O$, $\delta^{13}C$ Carbonate $\delta^{18}O$, $\delta^{13}C$	This study Palacios-Fest et al. (1993) and Cohen et al. (2000)
Limnocythere ceriotuberosa Wetlands Levee *Limnocythere ceriotuberosa*	1265 m	20 to >100 ka	Summer	Benthic, lacustrine	Carbonate $\delta^{18}O$, $\delta^{13}C$	Palacios-Fest et al. (1993) and Cohen et al. (2000)

Table 2
Average stable isotope values for carbonates and DIC in the Chewaucan lake system.

Sample material	Elevation range (m asl)	Average $\delta^{18}O \pm 1\sigma$ (‰ VPDB)	$\delta^{18}O$ range (‰ VPDB)	Average $\delta^{13}C \pm 1\sigma$ (‰ VPDB)	$\delta^{13}C$ range (‰ VPDB)	Source
Spring travertine	>1350 m	−14.0 ± 1.5	−17.1 to −12.8	−8.4 ± 1.4	−10.7 to −6.8	Jellinek et al., 1996
						This study
Shorezone tufa	1295–1346 m	−3.1 ± 1.3	−5.8 to −0.8	+3.5 ± 0.6	+1.9 to +4.5	Jellinek et al. (1996)
						This study
Spring mound tufa	1275–1312 m	−5.6 ± 0.8	−6.7 to −5.0	+1.5 ± 0.3	+1.0 to +1.9	Jellinek et al. (1996)
						This study
Vorticifex effusa shells	1302–1346 m	−2.4 ± 1.3	−4.6 to −0.6	−2.0 ± 1.8	−5.1 to +0.3	This study
Ana River Canyon *Limnocythere ceriotuberosa*	1280 m	−7.1 ± 1.8	−10.8 to −3.3	−2.1 ± 2.0	−5.5 to +2.8	Palacios-Fest et al. (1993), Cohen et al. (2000)
Wetlands Levee *Limnocythere ceriotuberosa*	1265 m	−5.2 ± 4.4	−23.7 to −2.4	−0.1 ± 2.8	−10.9 to +3.4	Palacios-Fest et al. (1993) and Cohen et al. (2000)
Abert Lake DIC	1295 m	−4.3	–	1.51	–	This study
Abert Rim spring DIC	1295 m	−13.7	–	−11.3	–	This study

(Table 3, S2). For shorezone tufas, we present Δ_{47} values and corresponding paleotemperature estimates (Table 4, S3) for recent (1.0 ka BP-present) and Late Glacial (18.4–14.2 ka BP) age samples from the Abert Lake sub-basin, constrained by ^{14}C ages (Table 5). There are four additional ^{14}C ages for shorezone and spring mound tufas, two ^{14}C ages for lake and spring water DIC (Table 5), and one U-Th series age (Table S4) for spring mound tufa, used to investigate reservoir effects and assess the potential for ^{14}C geochronology using carbonates.

5.1. Carbonate and DIC stable isotope results

Carbonates within the Chewaucan drainage basin have isotopic values ranging −10.9 to +4.5‰ (VPDB) for $\delta^{13}C_c$, and −23.7 to −0.8‰ for $\delta^{18}O_c$ (VPDB; Table 2). Individual carbonate types have separate and distinct ranges, but overall the values show strong positive covariance between $\delta^{13}C_c$ and $\delta^{18}O_c$ (Fig. 3). Isotope values for spring travertines (ranging −10.7 to −6.8‰ and −13.1 to −14.4‰ for $\delta^{13}C_c$ and $\delta^{18}O_c$, respectively; n = 8) are the lowest of any carbonate type. Isotope values for shorezone tufas (ranging +1.3 to +4.5‰ and −5.8 to −0.8‰ for $\delta^{13}C_c$ and $\delta^{18}O_c$, respectively; n = 40), are highest and tightly clustered. The values for the remaining carbonate types or phases (mollusks, ostracods, spring mound tufa, lake DIC) mostly fall between these two end members. Isotope values for sub-lake spring mound tufas (ranging +1.0 to +1.9‰ and −6.7 to −3.6‰ for $\delta^{13}C_c$ and $\delta^{18}O_c$, respectively; n = 10) exhibit weak within-group covariance possibly due to small sample size, and deviation of one sample from the Summer Lake sub-basin (CHL13-8; Table S1). Similar to the shorezone tufas, the range of variation in both isotopes is very small. Isotope values for mollusk shells and ostracods lie generally towards the high end of the observed range. *V. effusa* shells (ranging −5.1 to +0.3‰ and −4.6 to −0.6‰ for $\delta^{13}C_c$ and $\delta^{18}O_c$, respectively; n = 12), have $\delta^{18}O_c$ values within the same range as the tufas. However, their $\delta^{13}C_c$ values are scattered, and much lower than tufa values (Fig. 3). *L. ceriotuberosa* ostracod isotope values differ between the WL core (ranging −10.9 to +3.4‰ and −23.7 to −2.4‰ for $\delta^{13}C_c$ and $\delta^{18}O_c$, respectively; n = 43) and the ARC deposits (ranging −5.5 to +2.8‰ and −10.8 to −3.2‰ for $\delta^{13}C_c$ and $\delta^{18}O_c$, respectively; n = 59), a pattern also noted by previous investigators (Palacios-Fest et al., 1993). With the exception of five outlying values, ostracods from the WL core have a narrow range of $\delta^{13}C_c$ and $\delta^{18}O_c$ values that fall near the shorezone tufas. The outliers from the WL core have very low isotope values similar to those of the non-lacustrine spring travertines. In contrast to the WL ostracods, the isotope values from the ARC deposits are generally lower, and exhibit clear $\delta^{13}C_c/\delta^{18}O_c$ covariance. The highest $\delta^{13}C_c/\delta^{18}O_c$ values overlap with those from the WL core, and approach that of the tufas. However, the majority of values fall in the center of the trend between shorezone tufas and travertines. Finally, $\delta^{13}C_{DIC}/\delta^{18}O_{DIC}$ values for DIC of Abert Lake and Abert Rim spring water are similar to the shorezone tufa and travertine carbonates, respectively (Fig. 3, Table 1).

Table 3
Average stable isotope values for modern waters in the Chewaucan system and surrounding region.

Sample water	$\delta^{18}O$ (SMOW)	$\delta^{18}O$ (SMOW) Range	δD (SMOW)	δD Range (SMOW)	Source
Chewaucan system					
Summer Lake Wildlife Area well	−15.2	–	−117	–	Palmer et al. (2007)
Ana Reservoir	−13.7	–	−114	–	This study
Chewaucan River at Paisley	−14.5	–	−107	–	This study
Willow Creek	−13.6	–	−108	–	This study
Willow Creek pond	−9.9	–	−91	–	This study
Abert Rim Spring 1	−13.3	–	−109	–	This study
Abert Rim Spring 2	−13.9	–	−108	–	This study
Abert Lake	−6.7	–	−57	–	This study
Surrounding region	*Average values*		*Average values*		
Snowpack	−14.6	−16.8 to −13.2	−104	−119 to −93	Ingraham and Taylor (1989) and Palmer et al. (2007)
Streams	−14.4	−15.1 to −13.5	−104	−107 to −100	Ingraham and Taylor (1989) and Mariner et al. (1998)
Cold springs	−14.0	−15.6 to −13.2	−104	−115 to −94	Mariner et al. (1998) and Palmer et al. (2007)
Well waters	−13.5	−16.2 to −6.1	−107	−127 to −67	Sammel (1980), Mariner et al. (1998), Palmer et al. (2007)
Lakes	−4.3	−12.3 to +8.5	−49	−97 to +24	Sammel (1980), Ingraham and Taylor (1989) and Mariner et al. (1998)

5.2. Variation of carbonate isotopes with elevation and location

The $\delta^{13}C_c$ and $\delta^{18}O_c$ values for shorezone tufas, spring mound tufas, and shells have distinct patterns of variation, but in general do not show a clear trend with elevation for either isotope (Fig. 4). For shorezone tufas, $\delta^{13}C_c$ values display no significant change with elevation, and have similar values in both the Abert Lake and Summer Lake sub-basins (Fig. 4A). Spring mound tufas from the Abert sub-basin occur within a small range in both elevation (1307–1312 m asl) and $\delta^{13}C_c$ value (+1.0 to +1.9‰). A single spring mound tufa from the Summer Lake sub-basin (1275 m asl) has a similar $\delta^{13}C_c$ value. Shells exhibit no coherent variability in $\delta^{13}C_c$ with elevation, and span a large range (−4.0 to +0.3‰) at a single shoreline level (1322–1326 m asl).

Shorezone tufas exhibit distinct patterns of $\delta^{18}O_c$ values within similar elevation ranges, but do not show a consistent trend with changing elevation (Fig. 4B). Samples near the modern Abert Lake playa (<1300 m asl) yield the widest range and most negative values (−5.8 to −1.6‰). $\delta^{18}O_c$ values from middle shoreline levels in both sub-basins (1305–1337 m asl) are generally the highest (−3.2 to −0.8‰), while those from the highest shorelines (1340–1350 m asl), above the spilling threshold between the sub-basins, have intermediate values (−3.9 to −2.1‰). As with $\delta^{13}C_c$, spring mound tufas have lower $\delta^{18}O_c$ values with similar range (−6.7 to −5.1‰) compared to shorezone tufas at the same elevation. Shell $\delta^{18}O_c$ values are generally within the range of the shorezone tufas at the same elevation, except at one intermediate shoreline level (1322–1326 m asl).

5.3. Shorezone tufa clumped isotope results

Δ_{47} values for nine samples range from 0.640 ± 0.014 to 0.685 ± 0.011‰ (1 SE; 90 °C acid values, no acid fractionation correction; Fig. 6) for shorezone tufas collected from the Sheeplick Draw and Abert Rim areas (Figs. 1 and 2; Table 4). These correspond to temperatures ranging 3 ± 3 to 15 ± 4 °C (1 SE; Kelson et al., 2017). Each sampled tufa is paired with a ^{14}C age (detailed below) to constrain the age and confirm general contemporaneity of samples from each shoreline level. Three Late Holocene-age samples (CHL13-21, CHL15-31A, CHL15-70-2) from ~1296 m asl, on the modern Abert playa edge yield the highest temperatures of 11–15 °C (Fig. 6). Three samples of ~14 ka age (CHL13-2, CHL13-5, CHL13-29-1) from 1340 to 1346 m asl, yield variable temperatures of 3–14 °C. Three additional samples of ~18 ka age (CHL13-22, CHL14-30, CHL14-32-1) from ~1300 m asl, sampled on the Abert Rim just above the modern playa, yield consistent temperatures of 5–6 °C.

5.4. Water stable isotope results

Eight modern water $\delta^{18}O_w$ and δD values come from the southeastern edge of Abert Lake, the Chewaucan River, spring-fed Willow Creek, two springs discharging near the modern playa elevation from the Abert Rim, the Ana Reservoir, and groundwater from a well in the Summer Lake sub-basin (Palmer et al., 2007; Fig. 1; Table 3). Water $\delta^{18}O_w$ and δD range −6.7 to −15.2‰ and −57 to −117‰, respectively. Abert Lake water has the highest values, whereas inflowing streams and shallow

Table 4
Δ_{47} clumped isotope values and paleotemperatures for shorezone tufas in the Chewaucan lake system.

Sample ID	Elevation (m asl)	Sample site	Lake sub-basin	^{14}C age ± 2σ (cal yr BP)	Number of replicates	Δ_{47}	±1 SE[b]	T(Δ_{47}) Kelson (°C)[a]	±1 SE	$\delta^{13}C_c$ (‰ VPDB)	±1 SE[b]	$\delta^{18}O_c$ (‰ VPDB)	±1 SE[b]	$\delta^{18}O_w$ (‰ SMOW)[d]	±1 SE
CHL15-70-2	1295	Abert Rim	Abert Lake	Post-bomb	4	0.640	0.014	15	4	3.36	0.01	−5.20	0.02	−4.86	0.85
CHL13-21	1296	Abert Rim	Abert Lake	Post-bomb	6	0.646	0.016	14	4	4.10	0.06	−4.37	0.06	−4.35	0.86
CHL14-31A	1297	Abert Rim	Abert Lake	860 ± 70	4	0.656	0.014	11	4	3.87	0.01	−4.70	0.01	−5.33	0.88
Average of 'recent' replicates[c]					*14*	*0.650*	*0.007*	*13*	*2*						
CHL13-5	1346	Sheeplick Draw	Summer Lake	14,220 ± 190	6	0.645	0.011	14	3	3.29	0.02	−2.96	0.05	−2.89	0.65
CHL13-29-1	1340	Sawed Horn	Abert Lake	14,180 ± 340	4	0.669	0.014	7	4	3.56	0.01	−3.37	0.02	−4.78	0.90
CHL13-2	1346	Sheeplick Draw	Summer Lake	14,570 ± 330	6	0.685	0.011	3	3	3.38	0.01	−3.08	0.06	−5.46	0.70
CHL13-22	1299	Abert Rim	Abert Lake	17,720 ± 210	6	0.673	0.012	6	3	3.67	0.08	−3.59	0.04	−5.25	0.68
CHL14-30	1303	Abert Rim	Abert Lake	18,460 ± 210	4	0.677	0.014	5	4	1.89	0.02	−5.05	0.03	−6.93	0.91
CHL14-32-1	1301	Abert Rim	Abert Lake	18,060 ± 250	4	0.677	0.014	5	4	3.80	0.03	−3.49	0.01	−5.39	0.91
Average of 18 ka-age replicates[c]					*14*	*0.675*	*0.006*	*6*	*2*						

Italic terms represent the average of replicates of all samples in age group.

[a] Produced using Eq. (1) from Kelson et al. (2017): $\Delta_{47} = 0.0417(\pm0.0013) \times 10^6/T^2 + 0.139(\pm0.014)$.

[b] Calculated as standard error (SE) of the mean of all replicates as standard deviation of the replicates divided by the square root of the number of replicates.

[c] Combines all replicates of latest Holocene to modern 'recent' age or ca. 18 ka age based on similar age and sampling location of samples in each age group.

[d] Estimated lake water $\delta^{18}O$ composition for each sample, calculated using T(Δ_{47}), $\delta^{18}O_c$ and the calcite-water fractionation equation of Kim and O'Neil (1997).

Table 5
^{14}C ages for shoreline and spring tufas and DIC in the Chewaucan lake system.

Sample ID	AMS Lab ID	Sample type	Elevation (m asl)	Sample Site	Lake Sub-basin	$\delta^{13}C$ (‰ VPDB)	Fraction modern carbon[a]	^{14}C age $\pm 1\sigma$ (^{14}C yr BP)	^{14}C age $\pm 2\sigma$ (cal yr BP)
CHL13-29-1	AA105810	Shoreline tufa	1340	Sawed Horn	Abert Lake	3.6	0.217	12260 ± 40	14180 ± 340
CHL13-5	AA102250	Shoreline tufa	1346	Sheeplick Draw	Summer Lake	3.3	0.217	12270 ± 40	14220 ± 190
CHL13-2	AA104241	Shoreline tufa	1346	Sheeplick Draw	Summer Lake	3.4	0.213	12440 ± 40	14570 ± 330
CHL13-22	AA102261	Shoreline tufa	1299	Abert Rim	Abert Lake	3.7	0.164	14540 ± 70	17720 ± 210
CHL14-32–1	AA105971	Shoreline tufa	1301	Abert Rim	Abert Lake	3.8	0.157	14850 ± 90	18060 ± 250
CHL14-30	AA105816	Shoreline tufa	1303	Abert Rim	Abert Lake	1.9	0.151	15190 ± 80	18460 ± 210
CHL14-31A	AA105817	Shoreline tufa	1297	Abert Rim	Abert Lake	3.9	0.888	960 ± 30	860 ± 70
CHL13-21	AA102260	Shoreline tufa	1296	Abert Rim	Abert Lake	4.1	1.011	Post-bomb	Post-bomb
CHL15-49–2	AA106975	Shoreline tufa	1297	Abert Rim	Abert Lake	3.7	1.029	Post-bomb	Post-bomb
CHL15-68–2	AA106983	Shoreline tufa	1295	Abert Rim	Abert Lake	3.2	0.988	100 ± 20	140 ± 110
CHL15-70–2	AA106985	Shoreline tufa	1295	Abert Rim	Abert Lake	3.4	1.169	Post-bomb	Post-bomb
CHL13-1G	AA106994	Spring mound tufa	1312	Sawed Horn	Abert Lake	1.2	0.091	19240 ± 50[b]	–
CHL13-20	AA104466	Abert Rim Spring DIC	1295	Abert Rim	Abert Lake	-11.3	0.192	13230 ± 40[c]	–
CH13-24	AA104467	Abert Lake DIC	1295	Abert Rim	Abert Lake	1.5	1.068	Post-bomb	Post-bomb

[a] Ratio of ^{14}C in the sample to ^{14}C in the standard, where FMC = 1 corresponds in age to AD1950.
[b] Apparent ^{14}C age for spring mound tufa U-Th series dated to 20910 ± 270 cal yr BP (~17330 ± 80 ^{14}C yr BP).
[c] Apparent ^{14}C age for DIC of Abert Rim spring water collected May 2013.

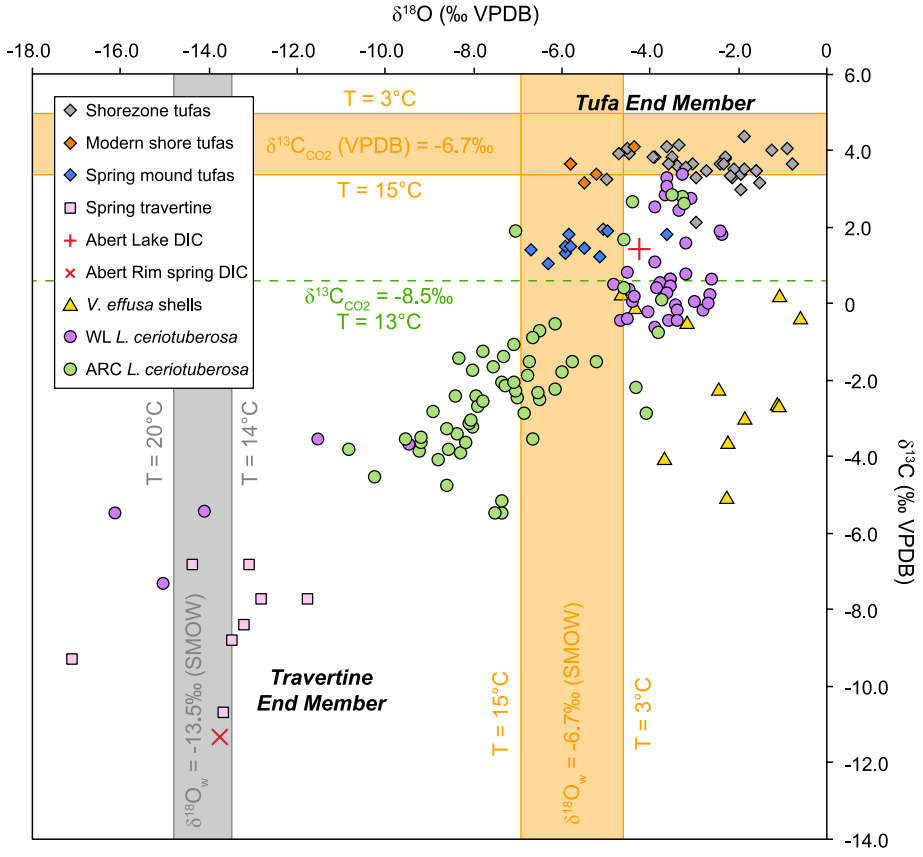

Fig. 3. $\delta^{18}O$ versus $\delta^{13}C$ biplot of carbonates and DIC for the Chewaucan lake system. Isotope values versus Vienna Pee Dee Belemnite. Samples are coded by carbonate type (see legend), with known modern shorezone tufas shown by orange diamonds. $\delta^{13}C_c$ value predicted by equilibrium fractionation (Mook et al., 1974) from modern (AD 2013) $\delta^{13}C_{CO2}$ of −8.5‰ at mean annual (13 °C) lake temperature shown by dashed green line. $\delta^{13}C_c$ value for shorezone tufas predicted by equilibrium fractionation from Late Glacial (−6.7‰) $\delta^{13}C_{CO2}$ at T(Δ_{47}) range 3–15 °C shown by horizontal orange lines. $\delta^{18}O_c$ value for shoreline tufas predicted for $\delta^{18}O_w$ of modern Abert Lake (−6.7‰) at 3–15 °C shown by vertical orange lines. $\delta^{18}O_c$ for travertines predicted from mean modern spring water (−13.5‰) $\delta^{18}O_w$ at modern regional spring water temperature of 14–20 °C shown by vertical gray lines.

groundwater are much lower (Fig. 5). In general, these isotope values are consistent with those from meteoric waters in the Upper Klamath Valley, adjacent to the western drainage divide of the Summer Lake sub-basin, and Surprise Valley, ~80 km south of Abert Lake (Sammel, 1980; Ingraham and Taylor, 1989; Mariner et al., 1998; Palmer et al., 2007). The values for the Chewaucan River at Paisley, OR, where it enters the Upper Chewaucan Marsh, fall along the global meteoric water line (GMWL; Craig, 1961), and are within the range of values for snow, streams, and springs (Ingraham and Taylor, 1989; Palmer et al., 2007), whereas those from Chewaucan springs show values consistent with regional springs and shallow well water. Samples of Willow Creek and Lake Abert water, fall below the GMWL, consistent with evaporation effects (Sammel, 1980; Ingraham and Taylor, 1989).

5.5. Dating results

Eleven ^{14}C ages for shorezone tufas range from post-AD 1950 to 15,190 ± 130 ^{14}C yr BP in age (Table 5). All samples with age control also have corresponding $\delta^{18}O_c/\delta^{13}C_c$ and/or clumped isotope values associated with them (Tables 2 and 4). Four young tufas sampled from the modern shoreline have fraction modern carbon (FMC) values of 0.988–1.169. One tufa sample from an older tufa layer on the same modern shoreline yielded an age of 860 ± 70 cal yr BP. Three tufas of late Last Glacial Maximum (LGM) age (17,720 ± 210 to 18,460 ± 210 cal yr BP) were collected from the Abert Rim from elevations 1299–1303 m asl, and three were sampled from the Late Glacial (14,180 ± 340 to 14,570 ± 330 cal yr BP) high shoreline elevations (1340–1350 m asl). A paired ^{14}C and U-Th series age for a single sample of spring mound tufa are 19,210 ± 130 ^{14}C yr BP and 20,910 ± 270 cal yr BP (Table S4), respectively.

Finally, two ^{14}C ages for Abert Lake and Abert Rim spring water DIC are post-AD 1950 and 13,240 ± 40 ^{14}C yr, respectively (Table 4), for which carbonate and water isotope values were also measured.

6. DISCUSSION

The combination of multiple carbonate stable and radiogenic isotope analyses presented here provides a basis for understanding the isotopic behavior of carbonate

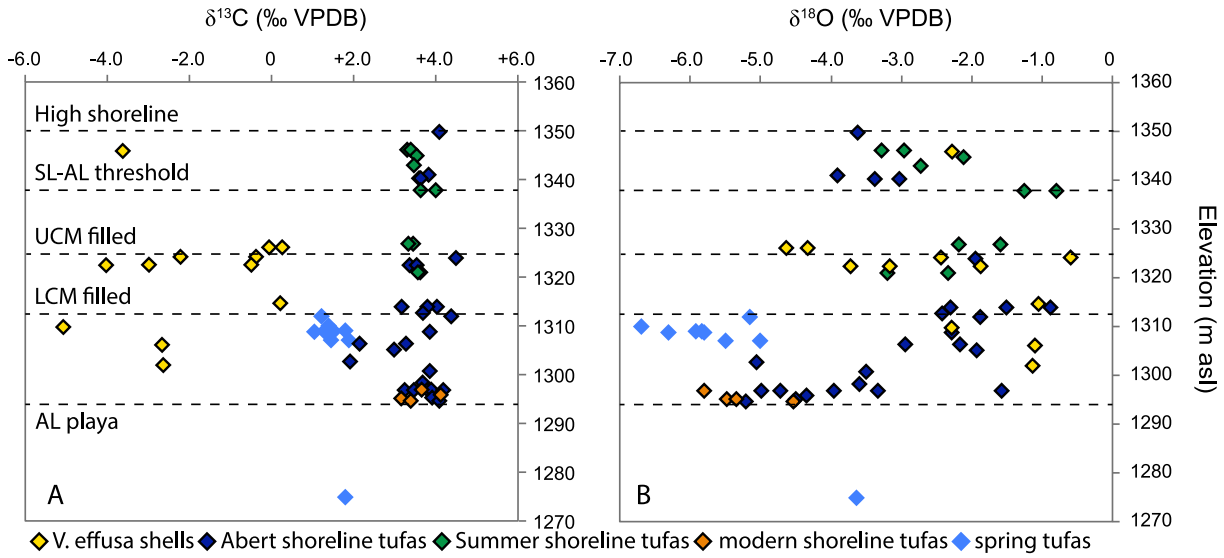

Fig. 4. Chewaucan tufa and shell $\delta^{18}O_c$ and $\delta^{13}C_c$ versus sampling elevation. Threshold elevations connecting individual sub-basins are indicated by dashed lines and labeled: high shoreline – highest Late Glacial-age shoreline, SL-AL threshold – spilling elevation connecting Summer Lake and Abert Lake sub-basins, UCM filled – threshold defining filling of Upper Chewaucan Marsh, LCM filled – threshold defining filling of Lower Chewaucan Marsh, AL playa – Abert Lake playa elevation. *V. effusa* shells shown by yellow diamonds, Abert sub-basin shorezone tufas by dark blue diamonds, Summer sub-basin shorezone tufas by dark green diamonds, modern shorezone tufas from the Abert playa by orange diamonds, and spring mound tufas by light blue diamonds. (For interpretation of the references to colour in this figure legend, the reader is referred to the web version of this article.)

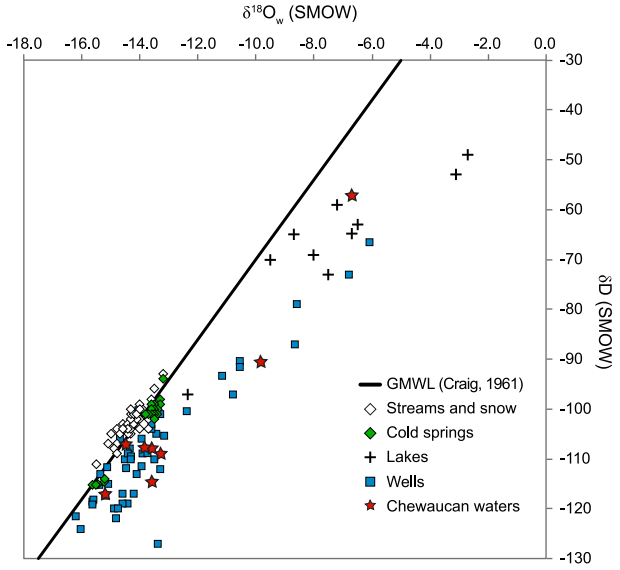

Fig. 5. Chewaucan modern water $\delta^{18}O_w$ and δD (red stars) compared with waters of the surrounding region. Global meteoric water line (GMWL; Craig, 1961) shown in black. Streams and snow shown by white diamonds; cold springs by green diamonds; lakes by black crosses; well waters by blue squares (data compiled from Sammel, 1980; Ingraham and Taylor, 1989; Mariner et al., 1998; Palmer et al., 2007). (For interpretation of the references to colour in this figure legend, the reader is referred to the web version of this article.)

precipitation in the Chewaucan lake system. This is vital for accurate reconstruction of past lake level, for identifying and quantifying sources of lake and spring water DIC, and for assessing the relationship between lake level and isotope composition. Discussion of the results is divided in four major sections. In the first section, we focus on shorezone tufas, by comparing the stable, clumped, and ^{14}C isotope compositions of modern lake DIC and tufas to expected modern values in isotopic equilibrium between atmospheric CO_2, lake water, the DIC pool, and lacustrine carbonate. In the second section, we use the constraints provided by the modern system to interpret the values and ages obtained for the fossil shorezone tufas to reconstruct past temperature for the northern Great Basin. In the third section, we assess the processes and DIC sources controlling the stable isotope compositions of all carbonates in the lake system, and their potential for reconstructing paleoenvironmental change. In the fourth section, we use the isotope dataset to interpret hydrologic variability for the Chewaucan lake system over the past 100 ka.

6.1. Shorezone tufas – A modern analog approach

Modern shorezone tufas are found on the east shoreline of Abert Lake, consisting of a thin (~1 mm) white layer of carbonate deposited extensively on fresh, lichen-free shoreline cobbles (Fig. 2F). This cobble beach is lower in elevation than the historic highstand of ~1298 m asl (AD 1958; Phillips and Van Denburgh, 1971), indicating it was deposited recently. This 'modern analog' material is a vital link for interpreting stable isotope values and ^{14}C ages for fossil tufas that are used in this and other studies (e.g. Ibarra et al., 2014; Petryshyn et al., 2016) as paleoclimate and lake level indicators.

Demonstrating the assumption that isotopic equilibrium is achieved between the gas, liquid, and solid phases in the

carbonate-forming system is key to reconstructing water and DIC isotope variations from fossil materials. Three possible sources of disequilibrium in carbonates are: kinetic fractionation of the DIC pool due to rapid degassing of CO_2 (e.g. Affek and Zaarur, 2014), disequilibrium between different DIC species ($CO_{2(aq)}$, HCO_3^-, CO_3^{2-}; e.g. Tripati et al., 2015), and disequilibrium due to mineral growth rate effects (Watkins and Hunt, 2015). Rapid degassing is not likely to occur in this case, because high pH lakes are generally neutral or net sinks for CO_2 (Duarte et al., 2008). Disequilibrium between DIC phases is also unlikely to occur, since the equilibration time required for a DIC pool at pH similar to Lake Abert is 10–15 days (Uchikawa and Zeebe, 2012), while the residence time of DIC in Lake Abert (calculated below) is years. Theoretical modeling of carbonate mineral formation (Watkins and Hunt, 2015) suggests most carbonates grown in laboratory experiments (e.g. Kim and O'Neil, 1997; Kelson et al., 2017), and in most natural settings, grow too quickly to achieve true isotopic equilibrium. However, laboratory-grown and most natural carbonates, including tufas, grow on comparable timescales (Watkins and Hunt, 2015), so laboratory-derived empirical relationships should provide reasonable approximations of the 'equilibrium' fractionation attained between the gas, liquid, and solid phases in most natural carbonate-forming systems. Both modeling and experimental data indicate Δ_{47} is unlikely to be strongly affected by this pH-dependent disequilibrium effect, so clumped isotope temperature estimates should be reasonably accurate, regardless of pH (Watkins and Hunt, 2015; Kelson et al., 2017). The pH of Lake Abert (9.7) is significantly higher than that in most carbonate precipitation experiments (generally ~ 8), but the predicted difference in effective fractionation factors for carbon and oxygen between pH 7 and 10 is <1‰ (Watkins and Hunt, 2015). This suggests tufa isotopic values can be used with laboratory-derived fractionation equations to calculate expected $\delta^{18}O_w$ and $\delta^{13}C_{DIC}$ for comparison to measured or estimated values. Based on this reasoning, it is unlikely that isotopic disequilibrium strongly affects our dataset or conclusions.

For the modern analog experiment, we first compare clumped isotope temperatures ($T(\Delta_{47})$) for modern shorezone tufas to measured lake surface temperatures to assess the seasonality of formation. We then constrain the ^{14}C reservoir effect for the modern and paleolake using a simple model for DIC mass balance and compare $\delta^{13}C_c$ and ^{14}C for shorezone tufas and lake DIC to expected values for isotopic equilibrium with the $\delta^{13}C$ and ^{14}C content of the atmosphere at $T(\Delta_{47})$.

6.1.1. $T(\Delta_{47})$ in recent Chewaucan tufas

$T(\Delta_{47})$ estimates from three recent tufas range from 11 ± 4 to 15 ± 4 °C (Fig. 6; Table 3). Compared to modern lake surface temperatures for Abert Lake, this range is consistent with formation at either mean annual temperature, or the spring or fall season (Fig. 7). It is too cold to reflect summer lake temperatures, in contrast to the findings of previous studies (Huntington et al., 2015; Petryshyn et al., 2015, 2016). For direct comparison, $T(\Delta_{47})$ of these tufas are significantly lower than those obtained for modern

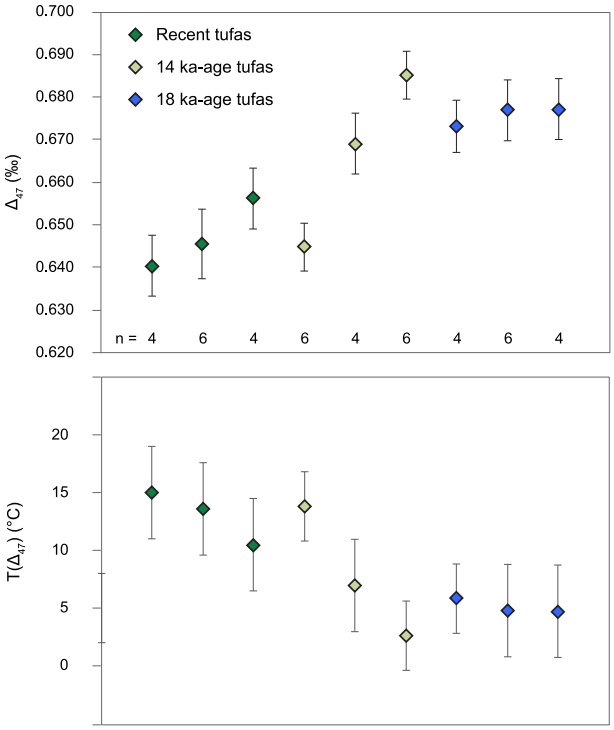

Fig. 6. Δ_{47} results and reconstructed temperatures ($T(\Delta_{47})$) for Chewaucan shoreline tufas. Δ_{47} values are shown as measured with a 90 °C reaction temperature, without acid fractionation correction. $T(\Delta_{47})$ is calculated using the calibration equation (Eq. (1)) of Kelson et al. (2017): $\Delta_{47} = 0.0417(\pm 0.0013) \times 10^6/T^2 + 0.139$ (±0.014). Recent tufas (modern – 0.9 ka BP) shown dark green; 14 ka-age highstand tufas shown in light green; 18 ka-age tufas shown in blue. All errors are 1 SE (Table 4). Number of replicates (n) for each sample shown beneath each symbol in the upper plot. (For interpretation of the references to colour in this figure legend, the reader is referred to the web version of this article.)

tufas from Walker Lake (26–30 °C), a closed basin lake at similar elevation, also in the Great Basin (Fig. 1; Petryshyn et al., 2016). This difference in temperature is too large to be an artifact of different ^{17}O corrections and Δ_{47}-temperature calibrations. Abert Lake and Walker Lake have similar pH, at 9.7 and 9.5, respectively, indicating the difference also cannot be explained by pH-dependent fractionation. This suggests a true difference in formation temperature.

The chemistry of waters in high pH salt lakes like the Chewaucan lake system may yield an explanation for the difference. Under modern conditions, the salinity of Lake Abert varies between 18,000 and 80,000 ppm (Phillips and Van Denburgh, 1971), and it is continuously supersaturated with respect to calcite. However, carbonate alkalinity ($HCO_3^- + CO_3^{2-}$) (~6,000–21,000 ppm) is at least three orders of magnitude higher than Ca^{2+} (<1.5 ppm), indicating that calcite precipitation is calcium limited. Although the overall salinity is much lower in the inflowing rivers and springs (~60–900 ppm), Ca^{2+} concentration is higher (~4–30 ppm), indicating that inflowing solutes provide the main source of calcium for carbonate formation. Coupled with the occurrence of significant tufa only near modern

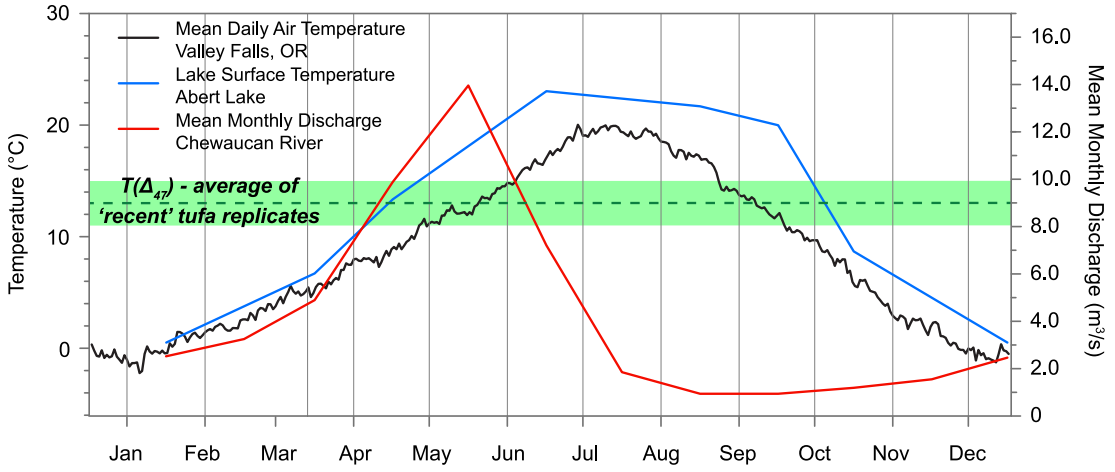

Fig. 7. Seasonal climate variation for the Chewaucan basin. Mean daily air temperature (black line, °C) for Valley Falls, OR was obtained using Climate Reanalyzer (http://cci-reanalyzer.org), Climate Change Institute, University of Maine, USA. Data are derived from the Global Historical Climatology Network daily average temperature for the Valley Falls station, AD 1930–2003 (www.ncdc.noaa.gov). Abert Lake surface temperature (blue line, °C) is based on spot measurements by Phillips and Van Denburgh (1971) AD 1956–57, 1961–63, averaged for each month. Some months have no observations, and data are linearly interpolated between months with observations. Chewaucan River discharge (red line, cubic meters per second) is a monthly average from the USGS stream gage near Paisley, OR, AD 1924–1991 (waterdata.usgs.gov). Average and 1 SE interval for $T(\Delta_{47})$ for all combined 'recent' (modern – 0.9 ka BP) tufas shown by dashed green line and light green band. (For interpretation of the references to colour in this figure legend, the reader is referred to the web version of this article.)

or paleo-spring discharge areas in the basin, this suggests significant carbonate formation occurs only where a steady supply of Ca^{2+} enters the lake. Therefore, tufa formation may be controlled by seasonal variation in discharge of Ca^{2+}-enriched inflows to the lake. This mechanism is known to drive marl deposition in other saline lakes worldwide (Katz and Kolodny, 1977; An et al., 2012).

Surface runoff in the Chewaucan watershed peaks during the late spring season, as evidenced by Chewaucan River discharge (Fig. 7). If Ca^{2+} delivery to the lake peaks with runoff, then tufa $T(\Delta_{47})$ could reflect late spring time temperatures. This mechanism is consistent with observations from Walker Lake, which is similarly calcium-limited, and where tufas may form interannually, only during summer seasons where exceptional river discharge brings sufficient Ca^{2+} to the lake (Petryshyn et al., 2012). Because local climate is quite similar between the two watersheds, however, this should not result in the observed formation temperature difference between the two lakes.

One key difference between the two lake systems is that Chewaucan tufas form only near spring outlets, suggesting that springs, not river discharge are the major source of Ca^{2+} for carbonate. Discharge in the spring-fed Ana River, like other cold springs in southern Oregon (Manga, 1997) varies by <50% during the year. The seasonal cycle of water discharge in the smaller springs is unknown, but is likely to behave similarly. If discharge and Ca^{2+} delivery is relatively constant, as in springs, then tufa may form year round, and $T(\Delta_{47})$ could instead reflect an annual average temperature. Based on the occurrence of tufa near spring outlets, and the temperature difference from Walker Lake tufas, we favor this mean annual tufa formation hypothesis. The microbialite textures of the shorezone tufas indicates algal photosynthesis may augment calcite formation during the warm season, but is likely not required for tufa formation around springs in calcium-limited lake systems like Chewaucan. These results indicate future studies reconstructing $T(\Delta_{47})$ using tufas should not assume that they record summer season temperatures without considering the hydrogeochemical setting of the lake.

6.1.2. Carbon isotopes in the modern and paleolake: outlook for carbonate ^{14}C dating

For the carbon isotope system, the consistent mean annual $T(\Delta_{47})$ in recent Chewaucan tufas can be used with $\delta^{13}C_c$ to calculate the expected DIC and CO_2 values from which they formed. This approach is most critical for constraining the potential ^{14}C reservoir effect in shorezone tufas, which can result from a combination of long DIC residence time and additions of ^{14}C-depleted carbon, which cause the DIC pool to have lower ^{14}C activity than the atmosphere. The extent of this effect in the past can be constrained by calculating the steady state mass balance of DIC (e.g. Peng and Broecker, 1980), if the ^{14}C activity of contributing sources is known, and the paleolake system behaves similar to the modern one. We estimate this mass balance for modern Lake Abert and use $\delta^{13}C$ and ^{14}C in modern materials for constraint, because both are tracers of DIC. ^{14}C is the most direct measure of reservoir effect, but $\delta^{13}C$ provides supporting constraint, and is a critical link for establishing similar system behavior between modern and fossil materials, because it does not change over time due to radioactive decay.

At hydrologic steady state (i.e. the size of the lake and DIC reservoirs is constant), the residence time of DIC is controlled by the fluxes of DIC coming from rivers, springs, and the atmosphere, relative to the size of the

Table 6
Water and dissolved inorganic carbon concentrations and fluxes for the Chewaucan lake system.

Water source	Shoreline elevation (m)[a]	Lake area (m^2)[a]	Water volume (m^3) or flux (m^3/yr)[a]	Volume/area[a]	DIC concentration (ppm)[b]	DIC concentration (mol/m^3)[c]	DIC reservoir or flux (mol/yr)	DIC FMC	Residence time (yr)	Reservoir age (yr)
Abert Lake	1297	1.48E+08	3.68E+08	2.49	9410	5.22	1.92E+09	0.998	2	9
Lake Chewaucan	1350	1.15E+09	5.85E+10	50.75	9410	5.22	3.06E+11	0.995	33	41
Chewaucan River	–	–	1.39E+08	–	46	0.026	3.56E+06	0.96	–	–
Abert Rim Springs	–	–	8.93E+06	–	253	0.14	1.25E+06	0.192	–	–
Ana River	–	–	8.04E+07	–	96	0.05	4.28E+06	–	–	–
CO_2 exchange rate[d]	–	–	–	–	–	–	1.19E+09	1	–	–

[a] Calculated using a digital elevation model of the Chewaucan basin derived from the 10 m National Elevation Dataset (Gesch et al., 2002).
[b] Calculated as the average of measurements made by Philips and Van Denburgh (1971) from AD1953-1963 at Abert Lake levels 1295.5–1298.5 m asl.
[c] Estimated as $[DIC]^* \rho_{H2O}/M_{H2O}$, where [DIC] is the fractional concentration of DIC in water (ppm/1×10^6), M_{H2O} is the molecular mass of H_2O (18.011 g/mol), and ρ_{H2O} is the density of H_2O (1 g/cm^3).
[d] Calculated using a CO_2 exchange flux of 8 mol/m^2 yr (Wanninkhof and Knox, 1996).

DIC reservoir. The steady state water balance for the lake can be expressed as:

$$Q_{riv} + Q_{spr} - E = 0 \quad (1)$$

where Q_{riv}, Q_{spr} and E are the water fluxes (m^3/s) for inflowing rivers, and springs, and outgoing evaporation, respectively. This assumes no significant water loss by groundwater seepage, which the solute mass balance study of Van Denburgh (1975) suggests is reasonable for this lake system. We estimate the DIC fluxes and reservoir size for Lake Abert using average DIC concentrations and water fluxes from Phillips and Van Denburgh (1971), measured between AD 1953 and 1963 (values listed in Table 6). For modern Lake Abert, we assume a lake level of 1297 m asl, similar to the historical average, and deep enough to submerge the modern tufas. This corresponds to a lake volume of 3.7×10^8 m^3. For steady state water balance, we assume the sum of river and spring discharge must equal an evaporation rate of 1.0 m/yr per unit surface area (m^2), based on direct monitoring of Lake Abert. Spring discharge, based on flow measurements, is estimated to be 8.93×10^6 m^3/yr. The remainder needed to balance evaporation yields a river water flux of 1.39×10^8 m^3/yr, (4.41 m^3/s), similar to average Chewaucan River discharge of ~4.25 m^3/s (Fig. 7). This suggests the assumption of hydrologic steady state is reasonable for modern conditions. The DIC reservoir in the lake (R_{lake}), and fluxes in spring (F_{spr}) and river (F_{riv}) input are then the product of the respective water volumes and concentrations. This yields values of 1.92×10^9 mol, 1.25×10^6 mol/yr, and 3.56×10^6 mol/yr, respectively (Table 6). The unit area DIC exchange flux with atmospheric CO_2 is estimated as 8 mol/m^2 yr, based on *in situ* measurements from several high-pH closed basin lakes in the Great Basin, including Walker Lake (Peng and Broecker, 1980; Wanninkhof and Knox, 1996), corresponding to a total flux (F_{atm}) of 1.19×10^9 mol/yr.

Based on these values, the atmospheric exchange flux is 2–3 orders of magnitude larger than that of rivers and springs (Table 6). It is similar in magnitude to the size of R_{lake}, making it the dominant control on residence time of DIC. At modern lake level, this residence time (R_{lake}/F_{atm}) is only ~2 yr. These calculations predict therefore that the DIC pool composition should be dominated by atmospheric exchange, and should respond within years to changes in the isotopic composition of atmospheric CO_2.

In addition to simple residence time, we can calculate the steady state FMC and ^{14}C reservoir age for Lake Abert following the equation (modified from Peng and Broecker, 1980):

$$F_{riv}\frac{(C_{riv} - C_{lake})}{C_{lake}} + F_{spr}\frac{(C_{spr} - C_{lake})}{C_{lake}} + F_{atm}\frac{(C_{atm} - C_{lake})}{C_{lake}} - R_{lake}\lambda_{14C} = 0 \quad (2)$$

where F_{riv}, F_{spr}, and F_{atm} are the fluxes of carbon in river, spring, and atmospheric input (mol/yr), C_{riv}, C_{spr}, C_{atm}, and C_{lake} are the FMC values for river DIC, spring DIC, atmospheric CO_2, and lake DIC, R_{lake} is the lake carbon reservoir (mol), and λ_{14C} is the decay constant for ^{14}C

(1/8032 yr). This expression states that the steady state ^{14}C balance for lake DIC is proportional to the sum of the flux-weighted FMC values coming from the drainage basin, atmosphere, and radiodecay. For this calculation we use F_{riv}, F_{spr}, F_{atm}, and R_{lake} values as above. We estimate FMC values for an idealized condition indexed to AD 1950, so that C_{atm} is equal to 1. C_{riv} is estimated as 0.96, based on the value for the pre-nuclear Walker River, which feeds Walker Lake (Peng and Broecker, 1980). We use this value since Chewaucan River FMC is unknown. C_{spr} is 0.192, the measured value for Abert Rim spring DIC. Solving for C_{lake} results in an FMC of 0.999, which corresponds to an effective reservoir age of 9 yr (Table 6). This value is significantly lower than reservoir ages measured or calculated for other high pH lakes in the Great Basin, Mono, Pyramid, and Walker, which range from ~100 to 1600 yr (Peng and Broecker, 1980; Broecker et al., 1988; Fig. 1), but consistent with a short DIC residence time, dominated by exchange with atmospheric CO_2.

These DIC and ^{14}C mass balance calculations indicating a small reservoir age are supported by $\delta^{13}C$ and ^{14}C data for modern materials. Abert Lake DIC, collected in May 2013, has a $\delta^{13}C_{DIC}$ value of +1.5‰ (Table 1; Fig. 3). This value is consistent with isotopic equilibrium (Mook et al., 1974) between the average atmospheric $\delta^{13}C$ value of −8.5‰ for 2013 measured at Humboldt State University (~380 km from the study area; White et al., 2015) at mean annual lake water temperature of 13 °C (Fig. 3). The $\delta^{13}C$ value of the atmosphere has decreased by ~1.8‰ over the past century due to fossil fuel addition (Rubino et al., 2013), so Abert Lake DIC in near equilibrium with a modern $\delta^{13}C$ value is consistent with the short DIC residence time predicted by the mass balance calculations. Similarly, Abert Lake DIC has an FMC of 1.068 (Table 5), a value similar to the post-AD 2000 atmosphere (Levin et al., 2013), consistent with a reservoir age close to zero. Therefore, both isotope systems indicate modern lake water DIC and atmospheric CO_2 are well mixed and in equilibrium.

Modern $\delta^{13}C_{DIC}$ of +1.5‰ should produce $\delta^{13}C_c$ values of ~+2.5‰ at isotopic equilibrium (Romanek et al., 1992), which is significantly less than the values for modern Abert Rim tufas (+3.2 to +4.5‰; Fig. 3; Table 2, S1). However, the tufas were likely formed over a period with a higher-than-modern atmospheric $\delta^{13}C$ value of −7.5 to −7.0‰ (Rubino et al., 2013), between when Abert Lake was last completely dry in the AD 1930s and the current dry period of AD 2014, when lake level was consistently higher than the sample elevations. This would result in an equilibrium $\delta^{13}C_c$ value of +3.5 to +4.0‰ at the mean modern T(Δ_{47}) of 13 °C, similar to that observed for the tufas.

The ^{14}C measurements for modern tufas are also consistent with minimal reservoir effect. Three of the four modern tufa samples dated have excess ^{14}C from nuclear testing ('bomb carbon', FMC of 1.011–1.169; Table 5). The remaining modern tufa sample (CHL15-68-2) has an FMC of 0.988, resulting in an apparent age of 140 ± 110 cal yr BP. The ^{14}C contents for the modern tufa is probably an average of carbonate formed over multiple decades between the present and the last time when Abert Lake was completely dry (circa AD 1930; Phillips and Van Denburgh, 1971). These tufas may therefore incorporate a variable range of atmospheric ^{14}C spanning this period, which may explain why they have slightly differing FMC between samples. On this and other samples all along the Abert Rim, we may also have inadvertently included some older tufa from a thin (~1 mm) sublayer of ~1.0 ka BP age (CHL14-31A), which underlies the modern material (Fig. 2F). In any case, the near-modern ages for all modern tufas provide further evidence that the DIC and shorezone tufa forming in modern Lake Abert is equilibrated with the atmosphere.

The key to assessing a reservoir effect for fossil tufas, which is critical for a paleolake level record, is that the DIC system behaves similarly in the past, and at high lake level. We estimate this using the same calculations for DIC balance and reservoir age used for the modern lake, and then compare to the $\delta^{13}C_c$ values of fossil tufas for additional support. For placing an upper bound on residence time and reservoir age, we estimate the carbon budget for the highstand lake level of 1350 m asl, when potential residence time was largest for the lake system. We again assume hydrologic steady state with a 1 m/yr evaporation rate to calculate the river and spring water inputs, no change in DIC concentration for the waters, and the same atmosphere exchange rate. For this deeper higher volume lake, DIC residence time increases to 33 yr (Table 6), due to the increase in R_{lake} relative to F_{atm}, proportional to the increase in volume/surface area of the lake. This suggests that even at high lake level, the DIC pool should respond quickly to changes in atmospheric CO_2. Calculating the reservoir effect using these fluxes and Eq. (2) yields a reservoir age of 41 yr, again suggesting that even at high lake level, the reservoir effect should be similar to the 1σ uncertainty in ^{14}C ages (Table 5), and is therefore negligible.

The $\delta^{13}C_c$ values for fossil tufas further support our interpretation of a low residence time dominated by exchange with atmospheric CO_2. The narrow range in $\delta^{13}C_c$ values for tufas at all elevations indicates they precipitated from a DIC reservoir with a relatively invariant composition that remained the same regardless of lake depth (Figs. 3 and 4). To test the conclusion that lake DIC was in equilibrium with atmospheric CO_2, we assume $\delta^{13}C_{CO2}$ ~ −6.7‰, the pre-industrial value (Schmitt et al., 2012). Using this value and the T(Δ_{47}) range for fossil tufas (3–15 °C), calculated calcite $\delta^{13}C_c$ values are ~+3.5 to +5‰, in close agreement with values from the majority of ancient shorezone tufas (Fig. 3). This provides additional evidence that Lake Chewaucan was well mixed with the atmosphere at high lake level. The sum of evidence from the mass balance calculations and the isotope measurements for modern and ancient materials therefore suggests ^{14}C dates on shorezone tufas should suffer from a negligible reservoir effect.

6.2. Reconstructing Late Glacial to recent temperature change in the northern Great Basin with tufas

The modern analog experiment clearly indicates that shorezone tufas past and present should yield reliable ^{14}C

ages, and their T(Δ_{47}) should reflect mean annual temperature, as long as tufa formation is controlled by localized discharge from springs. We therefore use the fossil shorezone tufas to place constraints on mean annual temperature change for the Chewaucan drainage basin and northern Great Basin since 18 ka BP, spanning the last deglaciation.

In addition to modern material, we analyzed a set of shorezone tufas of about 18 ka BP age from a shoreline just above the modern Abert playa (Table 4). The 18 ka-age tufas were sampled from similar locations along the Abert Rim, so they should reflect similar lake conditions to the recent-age samples. We therefore compare the T(Δ_{47}) for these two sets to reconstruct mean annual temperature change since 18 ka BP. Dating of maximum alpine glacier extents in western North America indicates temperature conditions similar to the LGM persisted as late as 16 ka BP (Young et al., 2011), so our temperature comparison should approximate LGM temperature change relative to modern conditions.

Within both the 18 ka and recent age groups, the Δ_{47} values are very consistent between sample means and all individual replicates, and the samples are very close in age and sampling elevation (Fig. 6; Table 4, S3). Based on this fact, we pool all replicates together from each group to reduce uncertainty through greater sample size (Table 3). Using this approach, T(Δ_{47}) for the ~18 ka-age tufas is 6 ± 2 °C (1 SE); lower than recent tufas at 13 ± 2 °C. The two groups have significantly different means using a two-sided student's t-test ($p = 0.016$). This comparison yields a mean annual water temperature difference of 7 ± 3 °C (1 SE). Temperature depression for LGM conditions of ~7 °C is consistent with estimates from western North America derived from terrestrial pollen (Worona and Whitlock, 1995), and from global climate, hydrologic and glacial modeling studies (Birkel et al., 2012; Ibarra et al., 2014; Barth et al., 2016). Unfortunately, the uncertainties in T (Δ_{47}) (±3 °C, 1 SE), preclude us from making a definitive independent temperature depression estimate based on our data. However, coupled with existing data, our results provide additional support for a 7 °C temperature change, and show promise for applying clumped isotope thermometry in tufas to paleoclimate studies.

In contrast, the T(Δ_{47}) results from the three high shoreline tufas of 14 ka age are variable (ranging 3–14 °C; Table 4), though intrasample replicate Δ_{47} variability is comparable to the 18 ka and recent tufas (Fig. 6; Table S3). The $\delta^{13}C_c$ and $\delta^{18}O_c$ values are also comparable (Table 4), providing no indication that these samples formed under disequilibrium conditions relative to the more consistent sets. There are two possible explanations for this discrepancy: either the high shoreline sample T (Δ_{47}) estimates reflect differing lake environments occurring coevally within the lake, or the tufas record real lake surface temperatures that capture the abrupt deglacial warming event at the onset of the Bølling/Allerød warm period.

There is potential that the high shoreline T(Δ_{47}) estimates simply reflect differing lake environments. The high shoreline samples were collected from three different locations in both the Sheeplick Draw (CHL13-2, 13-5) and Sawed Horn areas (CHL13-29-1), which could have had differing local temperatures at the specific locations where the tufas formed. They also have differing elevations (1346 m asl, and 1340 m asl), and there is no guarantee they were all formed at the same lake depth. Tufas in the high shoreline zone span elevations of 1338–1350 m asl (Fig. 4), suggesting variation in both lake depth, and depth of tufa formation may affect the temperatures they record. The low shoreline samples, on the other hand, must have formed in a shallow lake across a more restricted depth range. This suggests differences in lake temperature at different depths or areas within the lake may result in a range of temperatures recorded by shorezone tufas.

Conversely, the variability in T(Δ_{47}) in the 14 ka-age group is also broadly consistent with the abrupt transition to warmer climate conditions in the northern Great Basin region during the Bølling/Allerød warm period (Grigg and Whitlock, 1998; Licciardi et al., 2004; Briles et al., 2005; Daniels et al., 2005). The ages span the period 14.2–14.6 ka, which is coeval with the ~400 year transition from cold conditions during the Heinrich Event 1 stadial to the Bølling warm period, which are recorded throughout the northern hemisphere (Deplazes et al., 2013). Although the calendar age errors overlap, the oldest sample (CHL13-2) yields the coldest temperature (3 ± 3 °C), while the younger samples have the higher temperatures, consistent with an abrupt warming. Of these two explanations, we favor differences in formation environment as the more likely, given the variability in sample locations. More detailed analysis is required to determine whether these temperatures represent real climate change. Overall, it is clear that future studies utilizing shorezone tufas to reconstruct paleotemperature change should collect samples from similar inferred lake depths and locations to avoid possible environmental differences.

6.3. Carbonate isotope values as indicators of DIC provenance, lake environment, and paleoenvironmental change

The strong covariance in $\delta^{13}C_c$ and $\delta^{18}O_c$ values for all carbonate types in the study area is a commonly observed trend in closed-basin lake carbonates, reflecting the evolution from low isotopic values corresponding to inflowing meteoric water and DIC and high values caused by evaporative concentration (Fig. 3; Horton et al., 2016). While this covariance is often an indicator of closed basin conditions (Talbot, 1990), individual carbonate types in known closed basins often show weak or no covariance (e.g. Nelson et al., 2005; Ibarra et al., 2014; Horton et al., 2016), suggesting additional factors affect these materials. The same process which causes $\delta^{13}C_c/\delta^{18}O_c$ covariance is often the basis for using carbonate isotopes in paleoclimate records to infer changes in hydrologic budget through time (Benson et al., 1996b, 2003; Ibarra et al., 2014; Mishra et al., 2015; Petryshyn et al., 2016). In particular, $\delta^{18}O$ values of carbonates in closed-basin lakes are considered to reflect variations in the precipitation/evaporation (or runoff/evaporation) ratio of the catchment and lake (Leng and Marshall, 2004). Under this model, increased precipitation should increase runoff, adding water with a lower $\delta^{18}O_w$ value to

the lake, resulting in a lower lake $\delta^{18}O_w$ value. This should also result in an increase in lake level, area, and volume. Increased runoff may also lower $\delta^{13}C_{DIC}$ in the lake because of increased delivery of terrestrial carbon with low $\delta^{13}C$ value, resulting in covariance between the isotopes through time (Leng and Marshall, 2004). The opposite situation should result in a net increase in $\delta^{18}O_w$ and $\delta^{13}C_{DIC}$ and decrease in lake size. These hydrologic changes should be reflected in the isotopic composition of carbonates, allowing them to be reconstructed in paleoclimate records.

In this section, we argue that the covariance in $\delta^{13}C_c$ and $\delta^{18}O_c$ values for all carbonates in the Chewaucan system results from mixing of lake and terrestrial carbon end members, and not from changes in lake level by a simple runoff/evaporation mechanism. However, this mixing relationship is not consistently expressed between carbonate types or in different lake environments. Instead, the isotopic composition for each carbonate type reflects type- or location-specific effects, which make them difficult to compare to each other and are related to hydrologic change through different processes.

6.3.1. Shorezone tufas, travertines and spring mound tufas: evidence for two end member DIC mixing

Based on the modern analog experiment and mass balance calculations in Section 6.1, shorezone tufas appear to provide the best constraint on the isotope composition of lake water, defining a lake 'end member'. Their $\delta^{18}O_c$ values clearly record evaporated water conditions similar to modern $\delta^{18}O_w$, whereas their $\delta^{13}C_c$ values are consistent with DIC dominated by exchange with atmospheric CO_2. Within this carbonate type, no covariance between isotopes is observed. The travertines, which must have formed outside the lake, have the lowest $\delta^{18}O_c$ and $\delta^{13}C_c$ values, reflecting terrestrial DIC conditions. These low values characterize the water and DIC inputs to the lake before mixing with lake water, and modification by evaporation and CO_2 exchange (a terrestrial 'end member'). They also show no covariance. Intermediate to these end members, spring mound tufas have high $\delta^{13}C_c$ and $\delta^{18}O_c$ values, consistent with formation in an evaporated lake environment. They show no covariance, but are lower in both isotopes compared to the shorezone tufas, indicating they may form from a water and DIC mixture where spring water enters the lake bottom through fault-controlled discharge points. To test this, we define a two end member mixing model using the $\delta^{13}C_c$ and $\delta^{18}O_c$, and ^{14}C contents for the lake, and terrestrial end members, and then use the values for spring mound tufas to calculate the percentage of spring versus lake DIC contributing to their formation for each isotope.

$\delta^{18}O_c$ values of spring travertine in the Chewaucan system should be consistent with local meteoric $\delta^{18}O_w$ values. As a test, we compare the $\delta^{18}O_c$ values to modern $\delta^{18}O_w$ values. The $\delta^{18}O_w$ values of Abert Rim spring and Ana River water is consistent with values for springs, wells, streams and snow in the region (Table 3; Fig. 5), suggesting they are representative of meteoric water. Using the range of temperatures for springs in the Chewaucan basin (14–20 °C; Phillips and Van Denburgh, 1971), and the mean $\delta^{18}O_w$ value for Chewaucan springs (−13.5‰; Table 3) yields equilibrium calcite $\delta^{18}O_c$ values (−14 to −15‰) that are similar to spring travertines from the Chewaucan basin (Fig. 3). Because the exact age of the travertines, and how spring temperature may have changed in the past is unknown, any comparison beyond modern values is speculative.

Spring DIC $\delta^{13}C_{DIC}$ (−11.3‰) is too low to be derived wholly from atmospheric or volcanic CO_2 (Crater Lake, Oregon $\delta^{13}C_{CO2}$ value estimated at −7.4‰; James et al., 1999). Instead, this value indicates some mixing with soil CO_2 derived from C_3 plants (Smith and Epstein, 1971), which make up the bulk of the flora in the headwaters of the Abert Rim. The low ^{14}C content (FMC = 0.192) is also consistent with low ^{14}C contents of DIC for volcanically-influenced springs in the central Oregon Cascade Mountains (James et al., 1999). This low FMC is equivalent to an apparent age of 13,230 ± 40 ^{14}C yr BP and indicates that spring DIC is has a long residence time in local groundwater and mixes with volcanic CO_2.

For the mixing model, this means spring mound tufas formed by significant mixing with this reservoir should produce erroneously old ^{14}C ages. Although these mounds are not actively depositing today, we can compare the isotopic values and the offset between the U-Th series and ^{14}C ages for one spring mound tufa to estimate the percentage of spring and lake DIC in this material. If the $\delta^{13}C$, $\delta^{18}O$, and ^{14}C results in Lake Chewaucan carbonates can be interpreted in terms of a two end-member mixing system between DIC components, as indicated by the stable isotope covariance (Fig. 3), then all three isotopes should yield similar mixing proportions. To assess this, we calculate the percentage of spring DIC required to explain the spring mound tufa isotope values and reservoir effect as:

$$P_{spring} = \frac{I_{spt} - I_{lake}}{I_{spring} - I_{lake}} * 100 \quad (3)$$

where P_{spring} is the percent of spring-derived DIC, I_{spt} is the isotopic value for spring mound tufas, and I_{spring} and I_{lake} are the isotopic values for the travertine/spring DIC, and shorezone tufa/lake DIC end members, respectively. Eq. (3) is then calculated separately for $\delta^{13}C_c$ and $\delta^{18}O_c$ and FMC values and compared between the isotopes. We define the terrestrial and lake end members with a mean and standard deviation of the $\delta^{13}C_c$ and $\delta^{18}O_c$ values of the spring travertines and shorezone tufas, respectively (values listed in Table 2). The carbonate values are more suitable than those derived from the single DIC values for each end member because they provide a better measure of the full range of isotope variability, and modern lake DIC contains bomb carbon and is equilibrated with fossil-fuel influenced CO_2, which was not present when the spring tufa formed. Using the carbonate $\delta^{18}O_c$ values assumes that travertine and tufa carbonate phases were precipitated from water at similar temperatures, which seems reasonable given carbonate values consistent with formation from near mean annual temperature for both (Fig. 3). We assume the shorezone tufa end member has an FMC of 1.0 at the time of formation, and travertine end member has an FMC of 0.1926 ± 0.0011 (1σ), the theoretical pre-bomb modern lake value

and measured spring water DIC value, respectively. The U-Th series age for the spring mound tufa (20,910 ± 270 (2σ) cal yr BP) is similar to a ^{14}C age of 17,330 ± 80 (1σ) ^{14}C yr BP using the IntCal13 calibration curve (Reimer, 2013). Compared to the ^{14}C age measured for the same aliquot (19,240 ± 50 ^{14}C yr BP), the reservoir effect offset is 1910 ± 90 (1σ) ^{14}C years. This indicates that spring mound tufa incorporates some ^{14}C-deficient groundwater DIC along with lake DIC during carbonate formation. For I_{spr}, we use mean and standard deviation of values for $\delta^{18}O_c$ and $\delta^{13}C_c$ in spring mound tufas, and an FMC of 0.7883 ± 0.0088 (1σ), corresponding to the reservoir age of 1910 ± 90 ^{14}C years.

Calculating P_{spring} using Eq. (2) yields values of 16.8 ± 11.9% (2σ), 22.9 + 30.3/−22.9% and 26.2 ± 2.2% for $\delta^{13}C_c$, $\delta^{18}O_c$, and ^{14}C, respectively (Fig. 8). P_{spring} overlaps at 2σ for all three isotopes. ^{14}C has the smallest range of possible values because it is based on a single sample measurement. However, $P_{spring} < 20.3\%$ is not permitted by the data, even if the DIC end-member ^{14}C content is assumed to be ^{14}C-dead (i.e. FMC = 0). We therefore suggest the range of P_{spring} calculated using ^{14}C is not significantly in error. Because the $\delta^{13}C_c$ values for both the shoreline and spring mound tufas have lower variance compared to the $\delta^{18}O_c$ values, and the $\delta^{13}C_c$ value of the lake end member should be largely fixed by equilibrium with atmospheric CO_2, we favor the smaller range of P_{spring} indicated by $\delta^{13}C_c$, rather than that for $\delta^{18}O_c$. This results in an overlapping P_{spring} range between $\delta^{13}C_c$ and ^{14}C of 24.1–28.3%, which overlaps with the larger range for $\delta^{18}O_c$ (Fig. 8). Therefore, based on all three isotopes, the spring mound tufas incorporate 24–28% spring-derived DIC. The agreement in P_{spring} between the three isotope systems supports the conclusion that DIC is a two-end member mixing system for Lake Chewaucan. However, the isotope values of spring mound tufas represent a location-specific mixing effect that is not representative of the bulk lake water or DIC composition. With P_{spring} for $\delta^{18}O_c$, it is also an important distinction that this represents the proportion of DIC equilibrated with spring water, not the proportion of spring water. Because of the difference in DIC concentration between spring water and lake water (0.14 mol/m^3 and 5.22 mol/m^3, respectively; Table 6), the proportion of spring water is ~75% using a P_{spring} of 24–28%. This suggests the spring mounds were forming within a poorly mixed zone of mostly spring water at the underwater discharge points.

6.3.2. Isotope variability in skeletal biogenic carbonates

V. effusa and *L. ceriotuberosa* shells have $\delta^{13}C_c$ and $\delta^{18}O_c$ values that record lacustrine conditions, but like the spring mound tufas, they are influenced by location-specific effects within the lake environment. All mollusk shells and the WL core ostracods have $\delta^{18}O_c$ values that are broadly consistent with precipitation of carbonate from lake water of similar or more positive values relative to modern (Fig. 3; Tables 2 and 3). The $\delta^{13}C_c$ values for these two groups, however, are variable, and in general too negative to be consistent with equilibrium with modern lake DIC and/or pre-industrial atmospheric CO_2. The $\delta^{13}C_c$ of mollusk shells in particular has a large range that does not vary systematically with $\delta^{18}O_c$ or sampling elevation (Fig. 4). *V. effusa* are lung-breathing mollusks preferring rocky nearshore substrates where they feed on algae (Frest and Johannes, 1998). Their low $\delta^{13}C_c$ values likely reflect incorporation of some proportion of dietary carbon with low $\delta^{13}C$ (algae average ~−18‰ VPDB; Deines, 1980) into shell carbonate (McConnaughey and Gillikin, 2008). The remaining carbon is derived from water DIC, resulting in shell $\delta^{13}C_c$ values approaching that of the tufas, but more negative.

Similarly, the majority of ostracod valves from the WL core have $\delta^{13}C_c$ values that approach the tufas, but are more than 3‰ lower on average (Table 2). These more negative values may reflect a biological effect (Leng and Marshall, 2004) or formation from DIC with lower $\delta^{13}C_{DIC}$ than that of the epilimnion, due to the decay of ^{13}C-depleted organic matter in the benthic environment where these organisms live (Cohen et al., 2000). The $\delta^{13}C_c$ and $\delta^{18}O_c$ values for ARC ostracod valves differ significantly from those of the WL core, and deviate more than any other lacustrine carbonate group towards the terrestrial end member (Fig. 3). Because the same species of ostracod was sampled between both core locations, and they are coeval (constrained by tephrostratigraphy), a significant difference in formation environment must distinguish the two. Similar to the spring mound tufas, mixing with a large amount of spring water at the ARC location is expected, given the discharge point of the Ana River is <2 km upstream for the sampled sections (Fig. 1). Therefore, the more negative ARC ostracod values likely precipitated from very fresh, poorly mixed lake water.

Using the same mixing model for the ARC ostracods (Eq. (3)), but substituting the mean WL ostracod isotope values to represent the lake end member (Table 2), yields accordant P_{spring} values of 30.8 + 33.2/−30.8% (2σ) and 33.0 + 42.4/−33.0% for $\delta^{13}C_c$ and $\delta^{18}O_c$, respectively. This is greater than the P_{spring} values indicated for the spring mound tufas where carbonate formed directly atop the spring discharge points. This is particularly striking because of the large difference in DIC concentration between the lakes and incoming springs. The difference requires that for ARC ostracods with the lowest isotope values formed in ~100% Ana River water, perhaps in a low-density, fresh water cap atop saline lake water near the Ana River outlet.

With respect to interpreting paleohydrology, the strong covariance in ARC ostracod isotope values through the record led previous authors (Palacios-Fest et al., 1993; Cohen et al., 2000) to argue that underwater spring discharge from the Ana River outlet during high lake intervals resulted in a decrease in ARC ostracod isotope values. However, tufa isotope values from the Sheeplick Draw area, sampled from the highest Summer sub-basin shorelines that define lake areas encompassing the ARC deposits (Figs. 1 and 4), are consistently more positive ($\delta^{13}C_c$ = +3.3 to +4.0‰, $\delta^{18}O_c$ = −0.8 to −3.3‰). This indicates that even at high lake levels, the northern end of the Summer Lake sub-basin at times contained lake water with a highly evaporated and atmospherically-equilibrated composition, at least in the shorezone. Most ostracod isotope

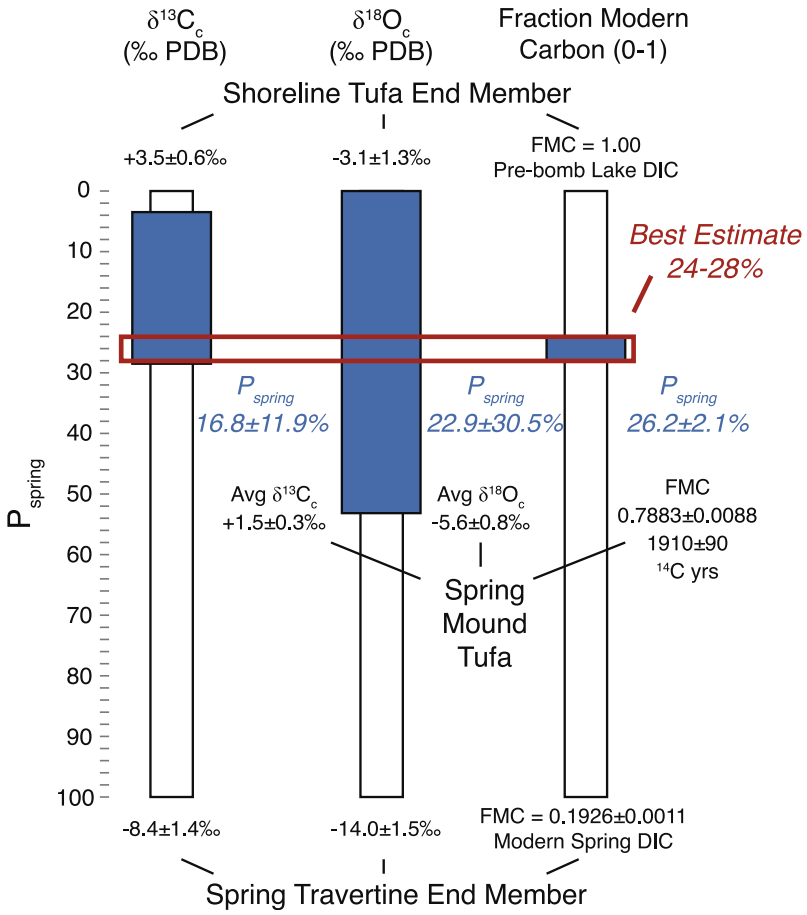

Fig. 8. Isotope-based mixing estimates for lake and spring-derived DIC in Chewaucan spring mound tufas. Shorezone tufa, spring travertine, and spring mound tufa stable isotope values shown are the average and one standard deviation of the observed carbonate values of each type. FMC values for each type are estimated as the theoretical 'modern' value for a pre-nuclear testing atmosphere, that measured in modern spring DIC and that for the observed reservoir effect of 1910 ± 90 ^{14}C yrs, respectively. The percent of spring-derived DIC (P_{spring}) estimated at 2σ for individual isotopes is shown by blue boxes. The best estimate of the percent contribution by springs, based on the overlap of all three isotopes, is shown by the bold red box. (For interpretation of the references to colour in this figure legend, the reader is referred to the web version of this article.)

values for the WL core, located near to the basin depocenter (Fig. 1), where they were deposited at significant depth within Summer Lake regardless of lake size, are consistent with the higher tufa values, although they do not overlap in age. Because the WL and ARC deposits are known to be deposited coevally, it is unlikely that a well-mixed lake encompassed both localities during their period of deposition. This therefore provides another example where location-specific effects control isotope variations, and it is not clear how this mixing relationship translates to lake level changes.

6.3.3. Oxygen isotopes in shorezone tufas: relationship between $\delta^{18}O_w$ and lake level

Beyond location-specific effects, another key difficulty with interpreting variations in past $\delta^{18}O_w$ inferred from carbonate $\delta^{18}O_c$ records is that increase/decrease in lake size and the corresponding changes in isotope composition may represent transient states, which can occur from a range of initial lake sizes and $\delta^{18}O_w$, and only persist while the hydrologic system has a positive or negative water balance (Steinman et al., 2010). Because of this, a range of $\delta^{18}O_w$ values can occur at a given lake level, complicating the relationship with $\delta^{18}O_w$. The $\delta^{18}O_c$ values for shorezone tufas in the Chewaucan lake system clearly show that low $\delta^{18}O_w$ does not correspond to high lake level. In fact, nearly the opposite pattern is observed (Fig. 4b). The lowest $\delta^{18}O_c$ values observed are for low elevation tufas deposited along the Abert Rim, while all of the fossil tufas both at similar and higher elevations have higher values. This relationship is counterintuitive, but is consistent with the effect of changing lake reservoir size on the magnitude of transient changes in $\delta^{18}O_w$ predicted from modeling (Steinman et al., 2010).

At a short scale, transient changes occur seasonally, as springtime runoff brings low-$\delta^{18}O_w$ water to the lake, lowering lake $\delta^{18}O_w$ and raising lake level, which then becomes higher as lake level declines during the summer due to evaporation (Benson, 1994; Steinman et al., 2010). Interannual to centennial-scale differences in seasonal discharge and

evaporation due to climate variability can produce more persistent changes in $\delta^{18}O_w$ of several per mil, which are recorded by carbonates, also accompanied by lake level change (Jones et al., 2005). All transient variability should be largest at low lake level, when lake volume is smallest relative to the seasonal water fluxes. At high, stable lake level, where lake size is large relative to inflows and outflows, transient isotope variations should become smaller, and on average approach a 'steady state' value where lake $\delta^{18}O_w$ is only a function of the difference between the inflowing water and the $\delta^{18}O_w$ of water vapor being removed (Steinman et al., 2010).

Shorezone tufas form in distinct elevation bands in this and many other lake systems (e.g. Lake Bonneville; Nelson et al., 2005), suggesting they formed under conditions of relatively stable lake level. Therefore, they may be biased towards recording $\delta^{18}O_w$ near a steady state value. However, the increase in variability at low lake level may make it more likely for tufas to record more variable and lower $\delta^{18}O_w$ conditions. This is consistent with the observed variability in $\delta^{18}O_c$ values of tufas at elevations near the Abert playa level (Fig. 4B). The most negative values come from the modern tufas, followed by the ~1.0 ka BP tufa layer underlying them at the same lake level (Fig. 2D). Based on their $T(\Delta_{47})$ and carbon isotope composition, shorezone tufas form year round at near isotopic equilibrium, and therefore should record mean annual lake $\delta^{18}O_w$. Modern tufa $\delta^{18}O_c$ (VPDB) values (avg. −5.2‰), are close to that predicted from equilibrium formation from water with the measured $\delta^{18}O_w$ value for modern Abert Lake (−6.7‰, VSMOW) at the measured $T(\Delta_{47})$ of ~13 °C (Fig. 3; Kim and O'Neil, 1997). However, the predicted $\delta^{18}O_w$ values for the recent-age Δ_{47} samples are still ~1.5‰ higher (Table 4), suggesting the measured Abert Lake $\delta^{18}O_w$ value, collected in May 2013, may be lower than the annual average due to freshening by springtime runoff. This is consistent with a spring season negative shift in lake water $\delta^{18}O_w$ (Steinman et al., 2010). Compared to the modern tufas, $\delta^{18}O_c$ values of fossil tufas from similar lake level are uniformly higher. The $T(\Delta_{47})$ results suggest at least some of the increase in $\delta^{18}O_c$ may result from higher isotopic fractionation at lower LGM water temperature. $\delta^{18}O_c$ values of tufas of ~18.0 ka age at low shoreline elevation (1300–1307 m asl) are ~2‰ higher than the late Holocene and modern samples. Using the $\delta^{18}O_c$ and $T(\Delta_{47})$ to calculate expected $\delta^{18}O_w$ values for both recent and 18 ka age sets of clumped isotope samples yields similar $\delta^{18}O_w$, consistent with differing fractionation (Table 4).

The fact that the most negative $\delta^{18}O_w$ values recorded by shorezone tufas occur at the lowest elevation is contrary to the prediction that low $\delta^{18}O_w$ should correspond to deeper lake conditions. However, tufas at low lake level may be more likely to have lower $\delta^{18}O_c$ simply because the transient shifts in hydrologic balance that occur at shallow depth are most likely to result in lower $\delta^{18}O_w$ values for the bulk lake. When lake depth is only a few meters, a negative water balance can easily cause the lake to dry in a matter of years. This rapid decline is unlikely to result in increased carbonate formation, since it is still limited by calcium supply in runoff. When the lake fills again, the water is likely to be relatively unevaporated, with a lower $\delta^{18}O_w$. If lake level continues to rise, even slowly, $\delta^{18}O_w$ will continue to be more negative than the steady state value, so that tufas and other carbonates formed under these conditions may be biased to record more negative values.

As shoreline elevation increases to moderate lake levels in both sub-basins (1307–1338 m asl), tufa $\delta^{18}O_c$ increases to values outside what can be explained by glacial-interglacial temperature change (Fig. 4B). This may reflect formation from a $\delta^{18}O_w$ closer to a steady state value. Above the threshold elevation, similar $\delta^{18}O_c$ values for highstand tufas from the northern ends of both sub-basins indicate similar conditions throughout the integrated lake, again reflecting $\delta^{18}O_w$ under stable lake conditions. The highstand shorezone tufas are lower in $\delta^{18}O_c$ than those from middle shoreline elevations (1305–1327 m asl), but are in the same range as those for Abert Lake tufas of ~18.0 ka BP age at ~1300 m asl elevation, indicating this $\delta^{18}O_c$ range is not unique to the lake highstand.

Other closed-basin lakes in the Great Basin also show relatively small ranges of $\delta^{18}O_c$ at a range of high lake levels, with no clear relationship to lake depth. Tufas from the Lake Bonneville system, located in the eastern Great Basin show an overlapping $\delta^{18}O_c$ range of about −2 to −6‰ (VPDB) between three different major shoreline levels with >100 m difference in lake depth (Nelson et al., 2005). Tufas from Lake Surprise, just south of Chewaucan, range −2.5 to −4.5‰ over ~100 m depth range, also with no trend in elevation (Ibarra et al., 2014). This provides further evidence that high $\delta^{18}O_w$ commonly develops at high lake level, and tufas may record these high 'steady state' isotope conditions.

We do not suggest that carbonate $\delta^{18}O$ records do not record transient hydrologic changes that have paleoenvironmental significance. Previous studies using ostracod $\delta^{18}O_c$ values in the WL and B&B cores found strong coherence between the isotope record and other sedimentologic and geochemical proxies for hydrologic budget change in the Summer Lake sub-basin (Cohen et al., 2000; Negrini et al., 2000; Benson et al., 2003). This is consistent with a transient response to an unbalanced hydrologic budget, resulting in change in both lake level and $\delta^{18}O_w$ of lake water. However, the shorezone tufas make it clear that negative (positive) $\delta^{18}O_c$ values do not necessarily correspond to deep (shallow) lake conditions, and other constraints are required for robust lake level reconstructions.

6.4. Constraints on lake level over the last 100 ka

Although lake level cannot be easily reconstructed from isotope variability, our results from multiple carbonates in the Chewaucan lake system provide some constraints on lake level variability over the past 100 ka. The large difference in isotope values between the coevally deposited WL and ARC ostracods suggests the north end of Summer Lake was often inundated by significant fresh water coming from the Ana River during the time interval ~20–100 ka. The paleohydrologic implication of the difference between the WL and ARC records is that Summer Lake was not significantly deeper than the Ana River discharge point

(1290 m asl) during the majority of the past 100 ka (Fig. 1). The density contrast between the Ana River and the saline lake would be maximized at low lake level, when salinity was highest (Fig. 9a). At high lake level, this density contrast would be less, and the Ana River spring outlet would discharge from the lake bottom at significant depth, making a large low density zone unlikely (Fig. 9b). Supporting this conclusion, shallow water conditions are generally indicated by the sedimentary facies in both the WL and ARC deposits for the majority of their respective depositional intervals, and previous authors concluded lake elevations >1315 m asl were unlikely (Cohen et al., 2000). This indicates that the extensive shoreline and littoral lake sediments, and shorezone tufas preserved on the basin margins up to the high shoreline levels above 1315 m asl, record hydrologically exceptional conditions that are missing from the ARC deposits. Consistent with this, tephrochronologic constraints indicate deposits dating to the Late Glacial period (17.8–11.7 ka BP) have been deflated from the ARC and WL sites. These deposits presumably would have recorded the basin integrating highstand (1340–1350 m asl) constrained by the tufas to 14.0–14.5 ka BP, and by dating of mollusk shells from 13 to 14 ka (Friedel, 2001; Licciardi, 2001). However, they were deflated during dry lake conditions of the middle Holocene, which created eolian dunes containing the 7.6 ka BP Mazama tephra deposited unconformably on the ARC canyon strata (Kuehn and Negrini, 2010).

These constraints on lake level indicate that, while colder, moister conditions characterized the northern Great Basin during the last glacial cycle (MIS 2-4; Cohen et al., 2000), lake level was modest. Even following

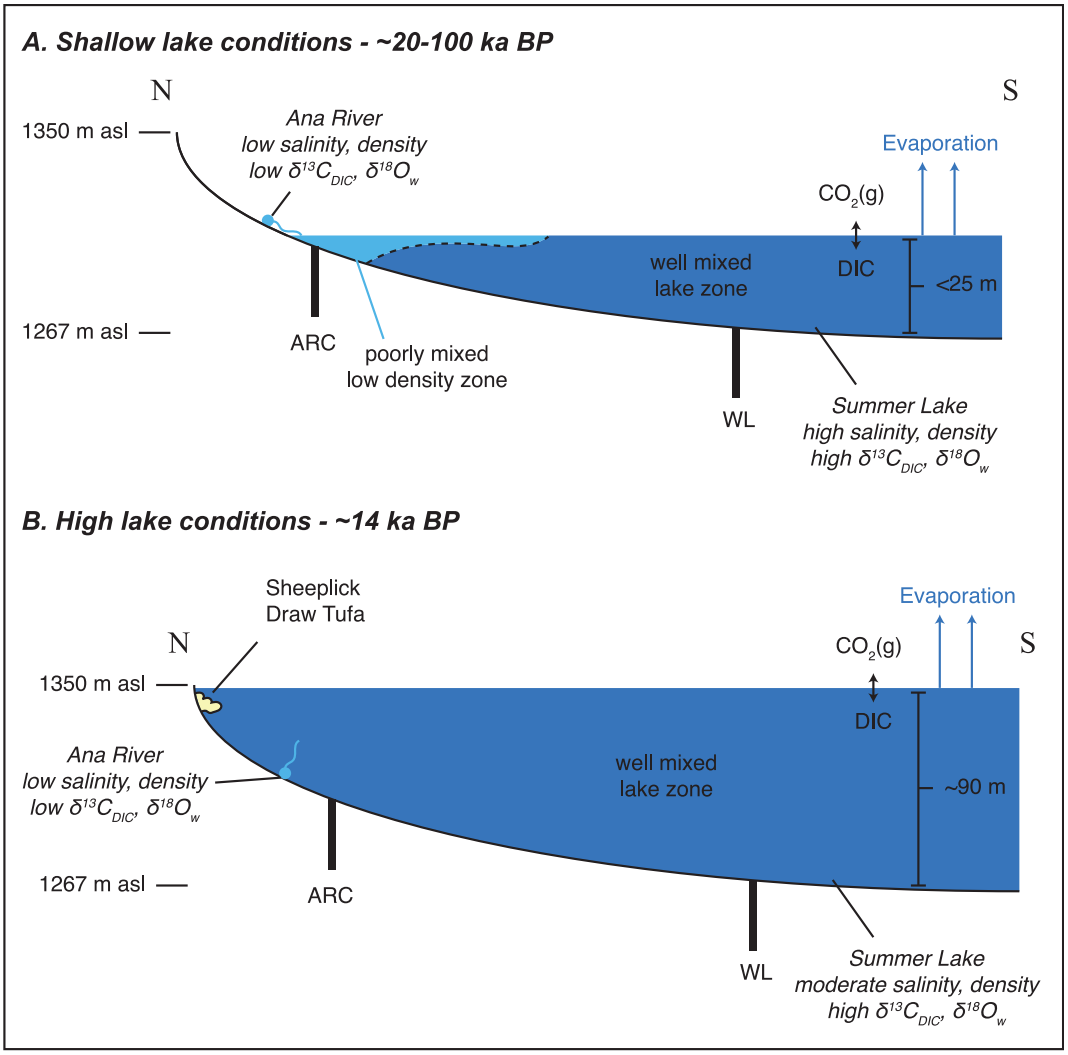

Fig. 9. Schematic cross-sections of the northern Summer Lake sub-basin showing proposed lake conditions at shallow and deep lake levels. Ana River and Summer Lake locations and contrasting geochemical conditions shown. Locations of key isotope sampling areas for ostracods (ARC – Ana River Canyon; WL – Wetlands Levee; Cohen et al., 2000) and shorezone tufas (this study) shown. Processes enriching isotope values in lake water (CO_2 exchange, evaporation) labeled schematically on right of diagram. (A) Shallow lake conditions recorded by the ARC and WL deposits (~20–100 ka BP), characterized by a low density shallow water zone over the ARC separated from a well mixed lake zone recorded over the WL core location. (B) Deep lake conditions recorded by the Sheeplick Draw tufas (~14 ka BP) characterized by a well-mixed, moderate density lake.

the maximum cold conditions of the LGM, the 18 ka-age tufas indicate Abert Lake level was similar to modern. The lake reached its highstand only briefly, from 13 to 14.5 ka, during the glacial termination. This evidence is consistent with other lakes in the Great Basin as well, where peak lake levels were mostly achieved during the deglacial interval (Munroe and Laabs, 2013). This suggests that relatively dry conditions characterize the mean climate state for the Great Basin during both glacial and interglacial periods, punctuated by short, but exceptionally wet intervals during deglaciation. Better defining the exact timing and cause for this exceptional wet interval is an area of ongoing research (e.g. Broecker and Putnam, 2013), which should improve understanding of the link between global climate change and hydrology in arid western North America.

7. SUMMARY AND CONCLUSIONS

Stable ^{18}O, ^{13}C and radioactive ^{14}C isotopes in closed-basin lake carbonates are commonly used reconstruct past hydrologic changes. We studied these isotopes in multiple carbonate materials within the Chewaucan lake system, including travertines, tufas, mollusk shells, and ostracods, to provide a clearer interpretation of the ages and paleoenvironmental record over the past 100 ka.

7.1. Implications for interpreting isotope data in closed basin lake systems

Overall, this study demonstrates that the specific hydrogeochemical setting contributes in complex ways to the behavior of carbonate isotopes in a closed-basin lake system. Our results for shorezone tufas show that modern tufa and lake DIC in the Chewaucan system have $\delta^{13}C$ values and ^{14}C ages consistent with a lake DIC budget dominated by equilibrium exchange with atmospheric CO_2, indicating there should be no reservoir effect for this material. $\delta^{13}C$ values for fossil tufas are also consistent with atmospheric equilibrium at all lake levels, suggesting these, and other materials formed in the lake epilimnion can dated reliably using ^{14}C. Clumped isotope thermometry of modern tufas indicates they form year round in response to a steady supply of Ca^{2+} delivered by springs discharging into the calcium-limited lake water, recording mean annual temperature conditions. This contrasts with previous research indicating tufas form during summer, suggesting the seasonality of formation should not be assumed when interpreting paleotemperature change.

$\delta^{13}C/\delta^{18}O$ covariance across all carbonate materials reflects mixing of non-lake water with low $\delta^{18}O$ and $\delta^{13}C$ values, and lake water and DIC with high values, defined by spring travertine and shorezone tufa end members, respectively. This mixing process is expressed differently depending upon carbonate type and local conditions in different parts of the lake system, and isotope variability cannot be reliably translated into lake level for any carbonates studied here. Modern shorezone tufas have $\delta^{18}O$ values consistent with modern Abert Lake water $\delta^{18}O$ values, but these values are most negative at low lake level, whereas those from higher shoreline levels indicate similar or more positive water $\delta^{18}O$ values. This further suggests that low (high) $\delta^{18}O$ does not always correspond to high (low) lake level. This is consistent with tufa data from other lake systems, and isotope budget modeling, showing a range of $\delta^{18}O$ can occur at any lake level, in response to transient changes in hydrologic budget.

7.2. Constraints on paleoclimate in northern Great Basin

The shoreline elevations and Δ_{47} temperatures for shorezone tufas spanning the LGM to present constrain the temperature and precipitation evolution in the northern Great Basin. Δ_{47} temperatures indicate tufas formed at mean annual lake temperature, with a 7 ± 3 °C (1 SE) difference between recent and LGM-age tufas, broadly consistent with previous estimates of glacial-interglacial temperature change. Dated shorezone tufas identify low lake level at 18 ka, and a prominent highstand at ~14 ka, consistent with previous dating of mollusk shells in shoreline deposits.

Although indirect evidence for lake level, $\delta^{13}C$ and $\delta^{18}O$ values for ostracods in the Ana River Canyon deposits suggest they formed in a very poorly mixed shallow water zone driven by high density contrast between saline Summer Lake and fresh Ana River water. This, in conjunction with other evidence, constrains Summer Lake to shallow depths during most of the past 100 ka. A deep pluvial Lake Chewaucan, such as that dated to ~14 ka by shorezone tufas here, was likely a consequence of unusually wet conditions that developed during the last glacial termination.

ACKNOWLEDGEMENTS

This work was funded by a Desert Research Institute Jonathan O. Davis Grant to AMH and Comer Science and Education Foundation grants to AMH and JQ. We thank David Dettman for providing help with stable isotope data acquisition for carbonates and waters at Arizona Isotope Lab facilities, and Alexis Licht and Andrew Schauer for assistance with clumped isotope data acquisition at UW Isolab. We thank Rich Cruz at Arizona AMS Lab for help with ^{14}C dating and Gary Skipp at the USGS for providing XRD analyses. We thank Lesleigh Anderson, Katie Snell, David McGee, Hagit Affek, and one anonymous reviewer for their comments that greatly improved this work. Any use of trade, product, or firm names is for descriptive purposes only and does not imply endorsement by the US Government.

APPENDIX A. SUPPLEMENTARY MATERIAL

Supplementary data associated with this article can be found, in the online version, at http://dx.doi.org/10.1016/j.gca.2017.06.024.

REFERENCES

Affek H. P. and Zaarur S. (2014) Kinetic isotope effect in CO_2 degassing: insight from clumped and oxygen isotopes in laboratory precipitation experiments. *Geochim. Cosmochim. Acta* **143**, 319–330.

Allison I. S. (1982) *Geology of Pluvial Lake Chewaucan, Lake County, Oregon*. Oregon State University Press, Corvallis, OR.

An Z., Colman S. M., Zhou W., Li X., Brown E. T., Jull A. J. T., Cai Y., Huang Y., Lu X., Chang H., Song Y., Sun Y., Xu H., Liu W., Jin Z., Lui X., Cheng P., Liu Y., Ai L., Li X., Liu X., Yan L., Shi Z., Wang X., Wu F., Qiang X., Dong J., Lu F. and Xu X. (2012) Interplay between the Westerlies and Asian monsoon recorded in Lake Qinghai sediments since 32 ka. *Nat. Sci. Rep.* **2**.

Barth C., Boyle D. P., Hatchett B. J., Bassett S. D., Garner C. B. and Adams K. D. (2016) Late Pleistocene climate inferences from a water balance model of Jakes Valley, Nevada (USA). *J. Paleolimnol.*. Available at: doi: http://dx.doi.org/10.1007/s10933-016-9897-z (Accessed August 8, 2016).

Benson L., Lund S., Negrini R., Linsley B. and Zic M. (2003) Response of North American great basin lakes to Dansgaard-Oeschger oscillations. *Quat. Sci. Rev.* **22**, 2239–2251.

Benson L. V. (1994) Stable isotopes of oxgyen and hydrogen in the Truckee River-Pyramid Lake surface-water system. 1. Data analysis and extraction of paleoclimate information. *Limnol. Oceanogr.* **39**, 344–355.

Benson L. V., Burdett J. W., Kashgarian M., Lund S. P., Phillips F. M. and Rye R. O. (1996a) Climatic and Hydrologic Oscillations in the Owens Lake Basin and Adjacent Sierra Nevada, California. *Science* **274**, 746–749.

Benson L., White L. D. and Rye R. (1996b) Carbonate deposition, Pyramid Lake Subbasin, Nevada: 4. Comparison of the stable isotope values of carbonate deposits (tufas) and the Lahontan lake-level record. *Palaeogeogr. Palaeoclimatol. Palaeoecol.* **122**, 45–76.

Birkel S. D., Putnam A. E., Denton G. H., Koons P. O., Fastook J. L., Putnam D. E. and Maasch K. A. (2012) Climate Inferences from a glaciological reconstruction of the late pleistocene Wind River ice cap, Wind River Range, Wyoming. *Arct. Antarct. Alp. Res.* **44**, 265–276.

Bonifacie M., Calmels D., Eiler J. M., Horita J., Chaduteau C., Vasconcelos C., Agrinier P., Katz A., Passey B. H., Ferry J. M. and Bourrand J.-J. (2017) Calibration of the dolomite clumped isotope thermometer from 25 to 350 C, and implications for a universal calibration for all (Ca, Mg, Fe)CO_3 carbonates. *Geochim. Cosmochim. Acta* **200**, 255–279.

Brady A. L., Slater G. F., Omelon C. R., Southam G., Druschel G., Andersen D. T., Hawes I., Laval B. and Lim D. S. S. (2010) Photosynthetic isotope biosignatures in laminated micro-stromatolitic and non-laminated nodules associated with modern, freshwater microbialites in Pavilion Lake, B.C. *Chem. Geol.* **274**, 56–67.

Brand W. A., Assonov S. S. and Coplen T. B. (2010) Correction for the ^{17}O interference in $\delta(^{13}C)$ measurements when analyzing CO_2 with stable isotope mass spectrometry (IUPAC Technical Report). *Pure Appl. Chem.* **82**. Available at: http://www.degruyter.com/view/j/pac.2010.82.issue-8/pac-rep-09-01-05/pac-rep-09-01-05.xml (Accessed August 29, 2016).

Bright J. and Kaufman D. S. (2011a) Amino acid racemization in lacustrine ostracodes, part I: effect of oxidizing pre-treatments on amino acid composition. *Quat. Geochronol.* **6**, 154–173.

Bright J. and Kaufman D. S. (2011b) Amino acids in lacustrine ostracodes, part III: Effects of pH and taxonomy on racemization and leaching. *Quat. Geochronol.* **6**, 574–597.

Briles C. E., Whitlock C. and Bartlein P. J. (2005) Postglacial vegetation, fire, and climate history of the Siskiyou Mountains, Oregon, USA. *Quat. Res.* **64**, 44–56.

Broecker W. S. and Kaufman A. (1965) Radiocarbon Chronology of Lake Lahontan and Lake Bonneville II, Great Basin. *Geol. Soc. Am. Bull.* **76**, 537–566.

Broecker W. S. and Putnam A. E. (2013) Hydrologic impacts of past shifts of Earth's thermal equator offer insight into those to be produced by fossil fuel CO_2. *Proc. Natl. Acad. Sci.* **110**, 16710–16715.

Broecker W. S., Wanninkhof R., Mathieu G., Peng T.-H., Stine S., Robinson S., Herzceg A. and Stuiver M. (1988) The radiocarbon budget for Mono Lake: an unsolved mystery. *Earth Planet. Sci. Lett.* **88**, 16–26.

Bronk Ramsey C. (2009) Bayesian analysis of radiocarbon dates. *Radiocarbon* **51**, 337–360.

Cheng H., Edwards R. L., Hoff J., Gallup C. D., Richards D. A. and Asmerom Y. (2000) The half-lives of uranium-234 and thorium-230. *Chem. Geol.* **169**, 17–33.

Cheng H., Edwards R. L., Shen C.-C., Polyak V. J., Asmerom Y., Woodhead J., Hellstrom J., Wang Y., Kong X., Spötl C., Wang X. and Calvin Alexander E. (2013) Improvements in 230Th dating, 230Th and 234U half-life values, and U-Th isotopic measurements by multi-collector inductively coupled plasma mass spectrometry. *Earth Planet. Sci. Lett.* **371–372**, 82–91.

Cohen A., Palacios-Fest M., Negrini R., Wigand P. and Erbes D. (2000) A paleoclimate record for the past 250,000 years from Summer Lake, Oregon, USA: II. Sedimentology, paleontology and geochemistry. *J. Paleolimnol.* **24**, 151–182.

Craig H. (1961) Isotopic variations in meteoric waters. *Science* **133**, 1702–1703.

Daëron M., Blamart D., Peral M. and Affek H. P. (2016) Absolute isotopic abundance ratios and the accuracy of Δ_{47} measurements. *Chem. Geol.* **442**, 83–96.

Daniels M. L., Anderson R. S. and Whitlock C. (2005) Vegetation and fire history since the Late Pleistocene from the Trinity Mountains, northwestern California, USA. *The Holocene* **15**, 1062–1071.

Defliese W. F., Hren M. T. and Lohmann K. C. (2015) Compositional and temperature effects of phosphoric acid fractionation on Δ_{47} analysis and implications for discrepant calibrations. *Chem. Geol.* **396**, 51–60.

Deines P. (1980) The isotopic composition of reduced organic carbon. In *Handbook of Environmental Isotope Geochemistry, The Terrestrial Environment A*, vol. 1 (eds. P. Fritz and J. C. Fontes). Elsevier, Amsterdam, pp. 23–406.

Dennis K. J., Affek H. P., Passey B. H., Schrag D. P. and Eiler J. M. (2011) Defining an absolute reference frame for "clumped" isotope studies of CO_2. *Geochim. Cosmochim. Acta* **75**, 7117–7131.

Dennis K. J. and Schrag D. P. (2010) Clumped isotope thermometry of carbonatites as an indicator of diagenetic alteration. *Geochim. Cosmochim. Acta* **74**, 4110–4122.

Deplazes G., Lückge A., Peterson L. C., Timmermann A., Hamann Y., Hughen K. A., Röhl U., Laj C., Cane M. A., Sigman D. M. and Haug G. H. (2013) Links between tropical rainfall and North Atlantic climate during the last glacial period. *Nat. Geosci.* **6**, 213–217.

Duarte C. M., Prairie Y. T., Montes C., Cole J. J., Striegl R., Melack J. and Downing J. A. (2008) CO_2 emissions from saline lakes: a global estimate of a suprisingly lare flux. *J. Geophys. Res. Atmospheres* **113**, G04041.

Eagle R. A., Eiler J. M., Tripati A. K., Ries J. B., Freitas P. S., Hiebenthal C., Wanamaker A. D., Taviani M., Elliot M., Marenssi S., Nakamura K., Ramirez P. and Roy K. (2013) The influence of temperature and seawater carbonate saturation state on ^{13}C–^{18}O bond ordering in bivalve mollusks. *Biogeosciences* **10**, 4591–4606.

Eiler J. M. (2007) "Clumped-isotope" geochemistry—The study of naturally-occurring, multiply-substituted isotopologues. *Earth Planet. Sci. Lett.* **262**, 309–327.

Eiler J. M. (2011) Paleoclimate reconstruction using carbonate clumped isotope thermometry. *Quat. Sci. Rev.* **30**, 3575–3588.

Frest T. J. and Johannes E. J. (1998) Freshwater Mollusks of the Upper Klamath Drainage, Oregon. *USDI Bur. Reclam. Rep.*, 402 p.

Friedel D. (2001) Pleistocene Lake Chewaucan: two short pieces on hydrological connections and lake-level oscillations. In *Quaternary Studies near Summer Lake, Oregon* Friends of the Pleistocene Field Trip Guide.

Gasse F., Arnold M., Fontes J. C., Fort M., Gibert E., Huc A., Li B., Li Y., Qing L., Melieres F., Van Campo E., Want F. and Zhang Q. (1991) A 13,000-year climate record from western Tibet. *Nature* **353**, 742–745.

Gasse F., Fontes J. C., Van Campo E. and Wei K. (1996) Holocene environmental changes in Bangong Co basin (Western Tibet). Part 4: Discussion and conclusions. *Palaeogeogr. Palaeoclimatol. Palaeoecol.* **120**, 79–92.

Gesch D., Oimoen M., Greenlee S., Nelson C., Steuk M. and Tyler D. (2002) The National Elevation Dataset. *Photogramm. Eng. Remote Sens.* **68**, 5–11.

Ghosh P., Adkins J., Affek H., Balta B., Guo W., Schauble E. A., Schrag D. and Eiler J. M. (2006) ^{13}C–^{18}O bonds in carbonate minerals: a new kind of paleothermometer. *Geochim. Cosmochim. Acta* **70**, 1439–1456.

Grigg L. D. and Whitlock C. (1998) Late-glacial vegetation and climate change in western Oregon. *Quat. Res.* **49**, 287–298.

Horton T. W., Defliese W. F., Tripati A. K. and Oze C. (2016) Evaporation induced ^{18}O and ^{13}C enrichment in lake systems: a global perspective on hydrologic balance effects. *Quat. Sci. Rev.* **131**, 365–379.

Hudson A. M., Quade J., Huth T. E., Lei G., Cheng H., Edwards L. R., Olsen J. W. and Zhang H. (2015) Lake level reconstruction for 12.8–2.3 ka of the Ngangla Ring Tso closed-basin lake system, southwest Tibetan Plateau. *Quat. Res.* **83**, 66–79.

Huntington K. W., Eiler J. M., Affek H. P., Guo W., Bonifacie M., Yeung L. Y., Thiagarajan N., Passey B., Tripati A., Daëron M. and Came R. (2009) Methods and limitations of "clumped" CO_2 isotope (Δ_{47}) analysis by gas-source isotope ratio mass spectrometry. *J. Mass Spectrom.* **44**, 1318–1329.

Huntington K. W., Saylor J., Quade J. and Hudson A. M. (2015) High late Miocene-Pliocene elevation of the Zhada Basin, southwestern Tibetan Plateau, from carbonate clumped isotope thermometry. *Geol. Soc. Am. Bull.* **127**, 181–199.

Huth T., Hudson A. M., Quade J., Guoliang L. and Hucai Z. (2015) Constraints on paleoclimate from 11.5 to 5.0 ka from shoreline dating and hydrologic budget modeling of Baqan Tso, southwestern Tibetan Plateau. *Quat. Res.* **83**, 80–93.

Ibarra D. E., Egger A. E., Weaver K. L., Harris C. R. and Maher K. (2014) Rise and fall of late Pleistocene pluvial lakes in response to reduced evaporation and precipitation: evidence from Lake Surprise, California. *Geol. Soc. Am. Bull.* **126**, 1387–1415.

Ingraham N. L. and Taylor B. E. (1989) The effect of snowmelt on the hydrogen isotope ratios of creek discharge in Surprise Valley, California. *J. Hydrol.* **106**, 233–244.

Jaffey A. H., Flynn K. F., Glendenin L. E., Bentley W. C. and Essling A. M. (1971) Precision measurement of half-lives and specific activities of U 235 and U 238. *Phys. Rev. C* **4**, 1889–1906.

James E. R., Manga M. and Rose T. P. (1999) CO_2 degassing in the Oregon Cascades. *Geology* **27**, 823.

Jellinek A. M., Madin I. P. and Langridge R. (1996) Field and stable isotope indicators of geothermal resource potential, central Lake County, Oregon. *Or. Geol.* **58**, 3–9.

Jones M. D., Leng M. J., Roberts C. N., Turkes M. and Moyeed R. (2005) A coupled calibration and modelling approach to the understanding of dry-land lake oxygen isotope records. *J. Paleolimnol.* **34**, 391–411.

Katz A. and Kolodny Y. (1977) The geochemical evolution of the Pleistocene Lake Lisan-Dead Sea system. *Geochim. Cosmochim. Acta* **41**, 1609–1626.

Kele S., Breitenbach S. F. M., Capezzuoli E., Meckler A. N., Ziegler M., Millan I. M., Kluge T., Deák J., Hanselmann K., John C. M., Yan H., Liu Z. and Bernasconi S. M. (2015) Temperature dependence of oxygen- and clumped isotope fractionation in carbonates: a study of travertines and tufas in the 6–95 C temperature range. *Geochim. Cosmochim. Acta* **168**, 172–192.

Kelson J. R., Huntington K. W., Schauer A. J., Saenger C. and Lechler A. R. (2017) Towards a universal carbonate clumped isotope calibration: diverse synthesis and preparatory methods suggest a single temperature relationship. *Geochim. Cosmochim. Acta* **197**, 104–131.

Kim S.-T. and O'Neil J. R. (1997) Equilibrium and nonequilibrium oxygen isotope effects in synthetic carbonates. *Geochim. Cosmochim. Acta* **61**, 3461–3475.

Kluge T., John C. M., Jourdan A.-L., Davis S. and Crawshaw J. (2015) Laboratory calibration of the calcium carbonate clumped isotope thermometer in the 25–250 C temperature range. *Geochim. Cosmochim. Acta* **157**, 213–227.

Kuehn S. C. and Negrini R. M. (2010) A 250 k.y. record of Cascade arc pyroclastic volcanism from late Pleistocene lacustrine sediments near Summer Lake, Oregon, USA. *Geosphere* **6**, 397–429.

Leng M. J. and Marshall J. D. (2004) Palaeoclimate interpretation of stable isotope data from lake sediment archives. *Quat. Sci. Rev.* **23**, 811–831.

Levin I., Kromer B. and Hammer S. (2013) Atmospheric Δ^{14} CO_2 trend in Western European background air from 2000 to 2012. *Tellus B* **65**. Available at: http://www.tellusb.net/index.php/tellusb/article/view/20092 (Accessed August 5, 2016)..

Licciardi J. M. (2001) Chronology of latest Pleistocene lake-level fluctuations in the pluvial Lake Chewaucan basin, Oregon, USA. *J. Quat. Sci.* **16**, 545–553.

Licciardi J. M., Clark P. U., Brook E. J., Elmore D. and Sharma P. (2004) Variable responses of western U.S. glaciers during the last deglaciation. *Geology* **32**, 81.

Lin J. C., Broecker W. S., Hemming S. R., Hajdas I., Anderson R. F., Smith G. I., Kelley M. and Bonani G. (1998) A reassessment of U-Th and ^{14}C ages for Late-Glacial high-frequency hydrological events at Searles Lake, California. *Quat. Res.* **49**, 11–23.

Manga M. (1997) A model for discharge in spring-dominated streams and implications for the transmissivity and recharge of Quaternary volcanics in the Oregon Cascades. *Water Resour. Res.* **33**, 1813–1822.

Mariner R. H., Evans W. C. and Huebner M. (1998) Preliminary Chemical and Isotopic Data for Waters from Springs and Wells on and near Medicine Lake Volcano, Cascade Range, Northern California. *US Geol. Surv. Open-File Rep.* **98–2**, 30.

McConnaughey T. A. and Gillikin D. P. (2008) Carbon isotopes in mollusk shell carbonates. *Geo-Mar. Lett.* **28**, 287–299.

McGee D., Quade J., Edwards R. L., Broecker W. S., Cheng H., Reiners P. W. and Evenson N. (2012) Lacustrine cave carbonates: novel archives of paleohydrologic change in the Bonneville Basin (Utah, USA). *Earth Planet. Sci. Lett.* **351–352**, 182–194.

Mishra P. K., Prasad S., Anoop A., Plessen B., Jehangir A., Gaye B., Menzel P., Weise S. M. and Yousuf A. R. (2015) Carbonate isotopes from high altitude Tso Moriri Lake (NW Himalayas) provide clues to late glacial and Holocene moisture source and

atmospheric circulation changes. *Palaeogeogr. Palaeoclimatol. Palaeoecol.* **425**, 76–83.

Mook W. G., Bommerson J. C. and Staverman W. H. (1974) Carbon isotope fractionation between dissolved bicarbonate and gaseous carbon dioxide. *Earth Planet. Sci. Lett.* **22**, 169–176.

Munroe J. S. and Laabs B. J. C. (2013) Temporal correspondence between pluvial lake highstands in the southwestern US and Heinrich Event 1. *J. Quat. Sci.* **28**, 49–58.

Negrini R., Erbes D., Faber K., Herrera A., Roberts A., Cohen A., Wigand P. and Foit F. (2000) A paleoclimate record for the past 250,000 years from Summer Lake, Oregon, USA. 1. Chronology and magnetic proxies for lake level. *J. Paleolimnol.* **24**, 125–149.

Nelson S. T., Wood M. J., Mayo A. L., Tingey D. G. and Eggett D. (2005) Shoreline tufa and tufaglomerate from Pleistocene Lake Bonneville, Utah, USA: stable isotopic and mineralogical records of lake conditions, processes, and climate. *J. Quat. Sci.* **20**, 3–19.

Palacios-Fest M. R., Cohen A. S., Ruiz J. and Blank B. (1993) Comparative paleoclimatic interpretations from nonmarine ostracodes using faunal assemblages, trace elements shell chemistry and stable isotope data. In *Geophysical Monograph Series* (eds. P. K. Swart, K. C. Lohmann, J. McKenzie and S. Savin). American Geophysical Union, Washington, D. C., pp. 179–190.

Palmer P. C., Gannett M. W. and Hinkle S. R. (2007) Isotopic characterization of three groundwater recharge sources and inferences for selected aquifers in the upper Klamath Basin of Oregon and California, USA. *J. Hydrol.* **336**, 17–29.

Peng T.-H. and Broecker W. S. (1980) Gas exhange rates for three closed-basin lakes. *Limnol. Oceanogr.* **25**, 789–796.

Petryshyn V. A., Corsetti F. A., Berelson W. M., Beaumont W. and Lund S. P. (2012) Stromatolite lamination frequency, Walker Lake, Nevada: implications for stromatolites as biosignatures. *Geology* **40**, 499–502.

Petryshyn V. A., Lim D., Laval B. L., Brady A., Slater G. and Tripati A. K. (2015) Reconstruction of limnology and microbialite formation conditions from carbonate clumped isotope thermometry. *Geobiology* **13**, 53–67.

Petryshyn V. A., Juarez Rivera M., Agić H., Frantz C. M., Corsetti F. A. and Tripati A. E. (2016) Stromatolites in Walker Lake (Nevada, Great Basin, USA) record climate and lake level changes ~35,000 years ago. *Palaeogeogr. Palaeoclimatol. Palaeoecol.* **451**, 140–151.

Pezzopane S. K. and Weldon R. J. (1993) Tectonic role of active faulting in central Oregon. *Tectonics* **12**, 1140–1169.

Phillips K. N. and Van Denburgh A. S. (1971) Hydrology and geochemistry of Abert, Summer, and Goose Lakes, and other closed-basin lakes in south-central Oregon. *U.S. Geol. Surv. Prof. Pap.* **502B**, 85.

Placzek C., Quade J. and Patchett P. J. (2006) Geochronology and stratigraphy of late Pleistocene lake cycles on the southern Bolivian Altiplano: implications for causes of tropical climate change. *Geol. Soc. Am. Bull.* **118**, 515–532.

Quade J., Eiler J., Daëron M. and Achyuthan H. (2013) The clumped isotope geothermometer in soil and paleosol carbonate. *Geochim. Cosmochim. Acta* **105**, 92–107.

Reichert K. L., Licciardi J. M. and Kaufman D. S. (2011) Amino acid racemization in lacustrine ostracodes, part II: Paleothermometry in Pleistocene sediments at Summer Lake, Oregon. *Quat. Geochronol.* **6**, 174–185.

Reimer P. (2013) IntCal13 and Marine13 Radiocarbon Age Calibration Curves 0–50,000 Years cal BP. *Radiocarbon* **55**, 1869–1887.

Romanek C. S., Grossman E. L. and Morse J. W. (1992) Carbon isotopic fractionation in synthetic aragonite and calcite: effects of temperature and precipitation rate. *Geochim. Cosmochim. Acta* **56**, 419–430.

Rubino M., Etheridge D. M., Trudinger C. M., Allison C. E., Battle M. O., Langenfelds R. L., Steele L. P., Curran M., Bender M., White J. W. C., Jenk T. M., Blunier T. and Francey R. J. (2013) A revised 1000 year atmospheric δ^{13} C-CO_2 record from Law Dome and South Pole, Antarctica: 1000 years of atmospheric $\delta^{13}C$-CO_2. *J. Geophys. Res. Atmospheres* **118**, 8482–8499.

Sammel E. A. (1980) Hydrogeologic appraisal of the Klamath Falls Geomthermal Area, Oregon. *US Geol. Surv. Prof. Pap.* **1044G**, 52 p.

Santrock J., Studley S. A. and Hayes J. M. (1985) Isotopic analyses based on the mass spectra of carbon dioxide. *Anal. Chem.* **57**, 1444–1448.

Schauer A. J., Kelson J., Saenger C. and Huntington K. W. (2016) Choice of ^{17}O correction affects clumped isotope (Δ_{47}) values of CO_2 measured with mass spectrometry: ^{17}O correction affects CO_2 clumped isotope. *Rapid Commun. Mass Spectrom.*. Available at: http://dx.doi.org/10.1002/rcm.7743 (Accessed November 2, 2016)..

Schmitt J., Schneider R., Elsig J., Leuenberger D., Lourantou A., Chappellaz J., Kohler P., Joos F., Stocker T. F., Leuenberger M. and Fischer H. (2012) Carbon isotope constraints on the deglacial CO_2 rise from ice cores. *Science* **336**, 711–714.

Smith B. N. and Epstein S. (1971) Two categories of $^{13}C/^{12}C$ ratios for higher plants. *Plant Physiol.* **47**, 380–384.

Steinman B. A., Rosenmeier M. F. and Abbot M. B. (2010) The isotopic and hydrologic response of small, closed-basin lakes to climate forcing from predictive models: simulations of stochastic and mean-state precipitation variations. *Limnol. Oceanogr.* **55**, 2246–2261.

Talbot M. R. (1990) A review of the palaeohydrological interpretation of carbon and oxygen isotopic ratios in primary lacustrine carbonates. *Chem. Geol.* **80**, 261–279.

Tang J., Dietzel M., Fernandez A., Tripati A. K. and Rosenheim B. E. (2014) Evaluation of kinetic effects on clumped isotope fractionation (Δ_{47}) during inorganic calcite precipitation. *Geochim. Cosmochim. Acta* **134**, 120–136.

Tripati A. K., Hill P. S., Eagle R. A., Mosenfelder J. L., Tang J., Schauble E. A., Eiler J. M., Zeebe R. E., Uchikawa J., Coplen T. B., Ries J. B. and Henry D. (2015) Beyond temperature: clumped isotope signatures in dissolved inorganic carbon species and the influence of solution chemistry on carbonate mineral composition. *Geochim. Cosmochim. Acta* **166**, 344–371.

Uchikawa J. and Zeebe R. E. (2012) The effect of carbonic anhydrase on the kinetics and equilibrium of the oxygen isotope exchange in the CO_2-H_2O system: Implications for $\delta^{18}O$ vital effects in biogenic carbonates. *Geochim. Cosmochim. Acta* **95**, 15–34.

Van Denburgh A. S. (1975) Solute Balance at Abert and Summer Lakes, South-Central Oregon. *U.S. Geol. Surv. Prof. Pap.* **502C**, 28.

Walker G. W. and Macleod N. S. (1991) Geologic Map of Oregon.

Wanninkhof R. and Knox M. (1996) Chemical enhancement of CO_2 exchange in natural waters. *Limnol. Oceanogr.* **41**, 689–697.

Watkins J. M. and Hunt J. D. (2015) A process-based model for non-equilibrium clumped isotope effects in carbonates. *Earth Planet. Sci. Lett.* **432**, 152–165.

Whitehead H. C. and Feth J. H. (1961) Recent chemical analyses of waters from several closed-basin lakes and their tributaries in the western United States. *Geol. Soc. Am. Bull.* **72**, 1421.

Worona M. A. and Whitlock C. (1995) Late Quaternary vegetation and climate history near Little Lake, central Coast Range, Oregon. *Geol. Soc. Am. Bull.* **107**, 867–876.

Young N. E., Briner J. P., Leonard E. M., Licciardi J. M. and Lee K. (2011) Assessing climatic and onclimatic forcing of Pinedale glaciation and deglaciation in the western United States. *Geology* **39**, 171–174.

Zaarur S., Affek H. P. and Brandon M. T. (2013) A revised calibration of the clumped isotope thermometer. *Earth Planet. Sci. Lett.* **382**, 47–57.

Zic M., Negrini R. M. and Wigand P. E. (2002) Evidence of synchronous climate change across the Northern Hemisphere between the North Atlantic and the northwestern Great Basin, United States. *Geology* **30**, 635.

Zimmerman S. R. H., Steponaitis E., Hemming S. R. and Zermeno P. (2012) Potential for accurate and precise radiocarbon ages in deglacial-age lacustrine carbonates. *Quat. Geochronol.* **13**, 81–91.

Associated editor: Hagit P. Affek